UNIVERSITÉ DE MONTRÉAL

PHYSICOCHEMICAL ANALYSES OF ALGINATES AND ALGINATE – POLY-L-LYSINE – ALGINATE MICROCAPSULES FOR THE IMPROVEMENT OF MICROCAPSULE BIOCOMPATIBILITY

SUSAN TAM

INSTITUT DE GÉNIE BIOMÉDICAL

ÉCOLE POLYTECHNIQUE DE MONTRÉAL

MÉMOIRE PRÉSENTÉ EN VUE DE L'OBTENTION
DU DIPLÔME DE MAÎTRISE ÈS SCIENCES APPLIQUÉES
(GÉNIE BIOMÉDICAL)
AOÛT 2004

© Susan Tam, 2004

Library and Archives Canada

Published Heritage Branch

395 Wellington Street
Ottawa ON K1A 0N4
Canada

Bibliothèque et Archives Canada

Direction du Patrimoine de l'édition

395, rue Wellington
Ottawa ON K1A 0N4
Canada

Your file Votre référence
ISBN: 0-612-97985-7
Our file Notre référence
ISBN: 0-612-97985-7

NOTICE:
The author has granted a non-exclusive license allowing Library and Archives Canada to reproduce, publish, archive, preserve, conserve, communicate to the public by telecommunication or on the Internet, loan, distribute and sell theses worldwide, for commercial or non-commercial purposes, in microform, paper, electronic and/or any other formats.

The author retains copyright ownership and moral rights in this thesis. Neither the thesis nor substantial extracts from it may be printed or otherwise reproduced without the author's permission.

AVIS:
L'auteur a accordé une licence non exclusive permettant à la Bibliothèque et Archives Canada de reproduire, publier, archiver, sauvegarder, conserver, transmettre au public par télécommunication ou par l'Internet, prêter, distribuer et vendre des thèses partout dans le monde, à des fins commerciales ou autres, sur support microforme, papier, électronique et/ou autres formats.

L'auteur conserve la propriété du droit d'auteur et des droits moraux qui protège cette thèse. Ni la thèse ni des extraits substantiels de celle-ci ne doivent être imprimés ou autrement reproduits sans son autorisation.

In compliance with the Canadian Privacy Act some supporting forms may have been removed from this thesis.

While these forms may be included in the document page count, their removal does not represent any loss of content from the thesis.

Conformément à la loi canadienne sur la protection de la vie privée, quelques formulaires secondaires ont été enlevés de cette thèse.

Bien que ces formulaires aient inclus dans la pagination, il n'y aura aucun contenu manquant.

Canada

UNIVERSITÉ DE MONTRÉAL
ÉCOLE POLYTECHNIQUE DE MONTRÉAL

Ce mémoire intitulé:

PHYSICOCHEMICAL ANALYSES OF ALGINATES AND ALGINATE – POLY-L-LYSINE – ALGINATE MICROCAPSULES FOR THE IMPROVEMENT OF MICROCAPSULE BIOCOMPATIBILITY

présenté par: TAM Susan
en vue de l'obtention du diplôme de: Maîtrise ès sciences appliquées
a été dûment acceptée par le jury d'examen constitué de:

M. CARTILIER Louis, Ph.D., président
M. YAHIA L'Hocine, Ph.D., membre et directeur de recherche
M. HALLÉ Jean-Pierre, M.D., membre et codirecteur de recherche
Mme FARÈ Silvia., Ph.D., membre

ACKNOWLEDGEMENTS

I would like to acknowledge the generous contributions of the many people who helped make this research project possible.

First of all, I would like to thank my research supervisor, Dr. L'Hocine Yahia, for without his support and guidance, this project would not have been possible. Not only did he provide the finances for the project, but he also provided the long-term vision that kept the project moving towards its goals. I am grateful for his patience and his willingness to take time out of his busy schedule to guide me through my research.

I would equally like to thank my co-supervisor, Dr. Jean-Pierre Hallé, for his leadership and his dedication to the improvement of the microencapsulation technique. I highly appreciate his ambitious attitude and his continual support, which were vital to the momentum of this project.

I would like to give many thanks to Stefania Polizu for being my advisor since day one of this project. Her intense dedication and generous advice have been invaluable to my understanding of many aspects of the research.

I would like to acknowledge the hours that Martin Ménard, Nathalie Henley, Guillaume Jourdain, and especially Julie Dusseault, have invested into researching and studying microcapsules at the CRGB. The results of their hard work contributed significantly to the experimental component of this project.

I would also like to thank several members of the Physics Department at the École Polytechnique for guiding me and helping me through many of the physicochemical analyses.

Finally, I am grateful to the Association Diabète Québec for the financial support and inspiration that they generously contributed.

ABSTRACT

The only treatment for insulin-dependent diabetes mellitus (IDDM) that can induce constant normoglycemia and insulin independence is the transplantation of a pancreas or of pancreatic cells. While whole pancreas transplantation is a high-risk procedure, islet cell transplantation is potentially a much safer and accessible treatment for IDDM.

By encapsulating the islet cells within a semi-permeable membrane, they can be protected from the immune system without the use of dangerous immunosuppressive medications. This approach to preventing graft rejection is termed microencapsulation. Microencapsulation consists of immobilizing the islet cells in an alginate-based gel, surrounding the gel bead with a semi-permeable layer of poly-L-lysine (PLL), and then coating the entire capsule with a biocompatible layer of alginate.

The microencapsulation technique is still in its stages of development, and its effectiveness as a treatment for IDDM in the absence of immunosuppression has not yet been clinically tested. Progress has mainly been hindered because the implanted microcapsules tend to induce a fibrotic overgrowth that leads to graft failure.

The exact causes for the immune reactions have not yet been identified. This is a general consequence of an inadequate knowledge of the physicochemical properties of the biomaterials. Specifically, current knowledge lacks in two areas: (1) Apart from proteins, endotoxins, and polyphenols, it is undetermined whether the alginates contain other immunogenic contaminants (2) Many chemical details regarding the microcapsule surface are ambiguous, including the degree of exposure of immunogenic PLL.

The general objective of this project was to explain the *in vivo* bioreactivity of the alginates and the microcapsules in terms of their physicochemical properties. The specific aims were to: (1) Identify and quantify the contaminants that are present in alginates after purification, (2) Evaluate the effect of these contaminants on the *in vivo* biocompatibility of the alginates, and (3) Determine the chemical composition of the microcapsule surface.

The study was designed in order to meet these objectives. Briefly, four purified alginates were studied: one was commercially purified, and three were chemically purified using different protocols. Crude alginate served as the control. The contaminants in the alginates were detected, identified, and quantified using the following techniques: Standard assays were applied to measure the protein, endotoxin, and polyphenol contents. Attenuated Total Reflectance Fourier Transform Infrared Spectroscopy (ATR-FTIR) and X-Ray Photoelectron Spectroscopy (XPS) were applied to detect, in an unbiased manner, the presence of all foreign elements and chemical groups. Viscometry, Differential Scanning Calorimetry (DSC), and the contact angle technique were applied to detect, in an indirect manner, the presence of contaminants by measuring their effects on the viscosity, thermal behaviour, and wettability of the alginates. Next, the effects of the contaminants on the *in vivo* biocompatibility of the alginates were evaluated. To do so, alginate gel beads were implanted into the peritoneal cavities of mice. After 2 and 14 days implantation, the foreign body reactions were evaluated in terms of the number of the immune cells that were floating in the peritoneal fluid, the number of immune cells that were adhered to the beads, and the degree of bead coverage by the adhering cells. Finally, the chemical composition of the microcapsule surface was determined using three techniques, each one having a different depth of analysis. These were ATR-FTIR, XPS, and Time-of-Flight Secondary Ion Mass Spectrometry (ToF-SIMS).

Despite purification, many contaminants were detected in the alginates. Specifically, proteins, endotoxins, and polyphenols were detected in all of the samples. Additionally, traces of sulphur and sodium contaminated the alginates. While the sodium-containing impurity could not be identified, the sulphur was presumed to originate from fucoidans. The samples also contained COOH groups that originated from proteins and/or insufficiently neutralized portions of the alginate. In total, as much as 7% of the alginate's atomic composition could be attributed to these contaminants.

The results strongly suggested that the identified contaminants contributed to the immunogenicity of the alginate gel beads. Specifically, the presence of proteins,

polyphenols, and, to a lesser extent, endotoxins appeared to promote the adhesion of immune cells to the bead surface. Plus, the presence of COOH groups in the alginate seemed to have a particularly potent effect on the severity of foreign body reactions. On the other hand, the presence of contaminating sulphur and sodium in the alginates had no obvious impact on bioreactivity of the implanted beads.

The evidence also suggested that the contaminants were indirectly contributing to immunogenicity of the beads. That is, the contaminants appeared to alter the conformation of the alginate molecules via bonds with the COO^- and C-OH groups, causing them to lose their flexibility, their ability to extend, and their hydrophilicity. As a result, the contaminants could have interfered with the alginate's natural abilities to resist the adsorption of proteins that promote cell adhesion to the bead surface.

It was repeatedly demonstrated that both PLL and alginate existed near the microcapsule surface. Within the outermost 100 Å of the microcapsules, the PLL molecules contributed to over 50% of the carbon and the remainder was attributed to alginate. Even the outermost monolayer of the microcapsule contained molecules and/or fragments of both alginate and PLL. Overall, the composition of the microcapsule surface was homogeneous, so PLL exposure was not due to defects in the outer alginate coating.

It was confirmed that, as a membrane component, the PLL was primarily bound to the alginate to form an alginate-PLL complex. The membrane PLL appeared to be in the α-helix and random coil conformations, and possibly in the β-sheet conformation as well. The evidence also supported the view that NH_3^+ groups of the PLL formed ionic bonds with the COO^- groups of the alginate. A portion of the surface alginate, however, retained its sodium ions and therefore may not have been bound to the PLL.

This project showed for the first time that, in addition to being contaminated by proteins, endotoxins, and polyphenols, alginates also contain previously undetected impurities. Moreover, this was the first clear demonstration that chemical purification does not completely remove these contaminants. Most importantly, there is evidence that these

residual contaminants have a profound effect on the *in vivo* biocompatibility of the alginates. Furthermore, it was discovered that contaminants alter the natural conformation and hydrophilic behaviour of alginate molecules. This led to the novel suggestion that, in addition to being immunogenic, the contaminants are capable of indirectly triggering an immune reaction by hindering the natural biocompatibility of the alginates.

Furthermore, this was the first time that the chemical composition of the outermost atomic layer of the microcapsules was directly investigated. As a result, this project provided the first physical evidence of PLL exposure at the true microcapsule surface.

Based on the new evidence, it is recommended that alginate biocompatibility be optimized using two approaches: The first approach is to completely eliminate all immunogenic impurities in the alginates. If this is to be attempted, it is suggested that physicochemical techniques, such as those that were used during this project, be used to ensure that the alginates are consistently free of all contaminants. The second approach is to counteract the effects of the contaminants on the alginate's properties. If the immunogenicity of the alginates is principally due to the altered conformation and hydrophilicity of the molecule, then it might not be necessary to eliminate 100% of the contaminants. A plasma treatment, for example, could be used to increase the hydrophilicity of the alginates enough to render the polymer fully biocompatible.

Based on the new evidence that PLL is in fact present at the microcapsule surface, it is justifiably recommended that efforts to better cover the PLL be continued. Because the PLL exposure doesn't appear to be due to defects or inadequate binding of the alginate coating, it is suggested that the thickness of the outer alginate layer be increased. This might be achieved by increasing the concentration of the alginate solution or by cross-linking the alginates to form a thick gel layer. Furthermore, it is advisable that new microcapsule designs be screened for PLL exposure using physicochemical techniques, such as XPS and ToF-SIMS, before implanting them into animals, as this approach would be most ethical and cost-efficient.

CONDENSÉ EN FRANÇAIS

L'introduction

Le seul traitement pour le diabète insulino-dépendant (DID) qui peut induire la normo-glycémie constante et l'indépendance d'insuline est la transplantation du pancréas ou des cellules pancréatiques. Tandis que la greffe d'un pancréas entier est considérée comme un procédé à haut risque, la transplantation de cellules des îlots de Langerhans est potentiellement moins risqué et plus accessible comme traitement pour le DID.

En encapsulant les îlots dans une membrane semi-perméable, ils peuvent être protégés contre le système immunitaire sans l'utilisation des médicaments immunosuppressifs dangereux. Cette approche pour empêcher le rejet de greffe, qui se nomme l'immunoprotection par la microencapsulation, est illustrée dans la Figure 1.

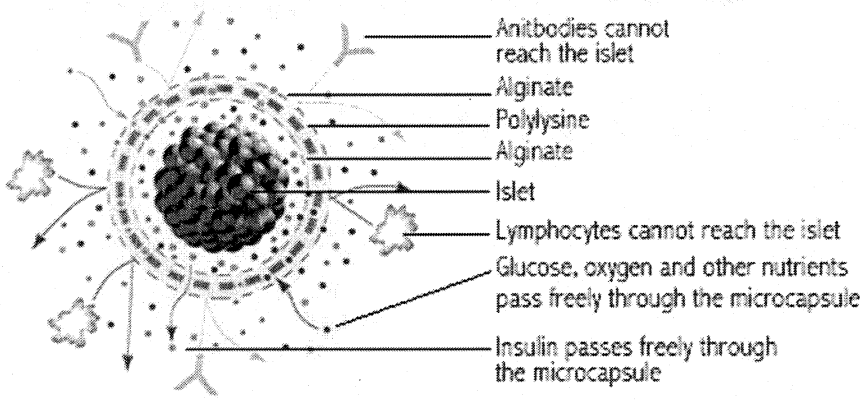


Figure 1 : Une illustration du concept de l'immunoprotection. Des îlots sont enfermés dans une microcapsule d'Alginate-Poly-L-lysine-Alginate (APA).

Brèvement, la microencapsulation consiste à immobiliser les îlots dans un gel d'alginate de calcium, à entourer la bille de gel avec une couche semi-perméable de poly-L-lysine (PLL), et puis à enrober la capsule entière d'une couche biocompatible composée d'alginate. Les structures chimiques de l'alginate de sodium et du bromhydrate de PLL sont illustrées dans la Figure 2.

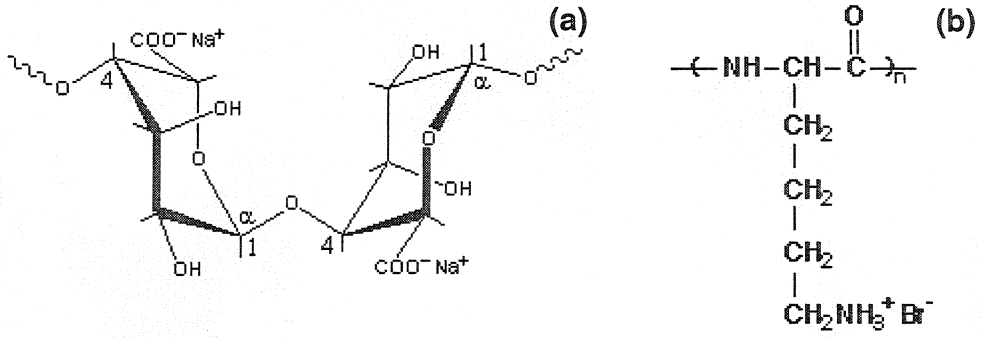


Figure 2 : La structure chimique **(a)** d'un bloc d'alginate de sodium formé de deux monomères d'acide guluronique (G), et **(b)** du bromhydrate de poly-L-lysine.

La technique de microencapsulation est toujours dans ses étapes du développement, et son efficacité comme traitement pour le DID en l'absence de l'immunosuppression n'a pas encore été testée cliniquement. Le progrès a été principalement gêné parce que les microcapsules implantées ont tendance à induire une surcroissance fibrotique qui mène à l'échec de la greffe. La prévention de cette réaction immunitaire contre les implants est donc primordiale pour la réussite de la technique de microencapsulation.

Le problème

Les causes de ces réactions immunitaires n'ont pas encore été identifiées avec précision. Ceci est une conséquence générale d'une connaissance insuffisante des propriétés physico-chimiques des biomatériaux. Spécifiquement, les connaissances actuelles sont déficientes en deux domaines : (1) En dehors des protéines, des endotoxines, et des polyphénols, il est indéterminé si les alginates contiennent d'autres contaminants qui sont immunogènes (2) Plusieurs détails chimiques concernant la surface de la microcapsule sont ambigus, y compris le degré d'exposition de PLL immunogène.

Les objectifs de recherche

L'objectif général de ce projet de recherche était d'expliquer la bioréactivité *in vivo* des alginates purifiés et des microcapsules en termes de leurs propriétés physico-chimiques.

Les objectifs spécifiques étaient de :

(1) Identifier et mesurer les contaminants qui sont présents dans l'alginate après la purification
(2) Évaluer l'effet de ces contaminants sur la biocompatibilité *in vivo* des alginates
(3) Déterminer la composition chimique de la surface de la microcapsule

Le raisonnement qui conduit à ces objectifs est le suivant : Premièrement, il y a une probabilité élevée que, en dépit de la purification, les alginates contiennent des impuretés immunogènes qui sont indétectables par des analyses courantes. En outre, l'assurance qu'il n'y a aucune impureté immunogène dans les alginates est un préalable à l'étude des effets d'autres propriétés sur la biocompatibilité, telles que le rapport de M/G. De plus, étant donné que la PLL est immunogène, il est impératif qu'elle n'entre pas en contact avec le tissu hôte. Il est donc essentiel de vérifier si la PLL est exposé à la surface de la microcapsule avant d'investir dans le développement de nouveaux designs.

La conception de l'étude

La sélection des alginates :
Quatre alginates purifiés ont été étudiés. L'un d'entre eux a été purifié par le manufacturier, et les trois autres ont étés purifiés chimiquement en suivant différents protocoles. L'alginate brut a servi comme contrôle.

La détection, l'identification, et la quantification des contaminants :
Les alginates ont été examinés *in vitro* pour la présence des impuretés. Des analyses courantes (la spectroscopie de fluorescence, le dosage par LAL, et le dosage par BCA) ont été appliquées pour mesurer les quantités de polyphénols, d'endotoxines, et de protéines, respectivement. Le ATR-FTIR et XPS ont été appliqués pour détecter la présence de tous les éléments et les groupements chimiques qui contaminaient les alginates. La viscométrie, le DSC, et l'angle de contact on été appliqués pour détecter,

d'une façon indirecte, la présence des impuretés en mesurant leur effet sur la viscosité, la réponse thermique, et la mouillabilité des alginates.

L'évaluation de la bioréactivité in vivo des alginates :
Pour évaluer la bioréactivité des alginates, des billes de gel d'alginate ont été implantées dans la cavité péritonéale des souris. Après 2 et 14 jours d'implantation, les souris ont été soumises à un lavage péritonéal. Les cellules immunitaires qui ont été attirées au site d'implantation ont été comptées, les cellules qui ont été adhérées aux billes ont été également comptées, puis la gravité des réactions péricapsulaires qui entouraient les billes ont été évalués par l'examen histologique. Les résultats des études *in vivo* ont été comparés à ceux des études *in vitro* afin de déterminer les corrélations entre les impuretés dans les alginates et les réactions induites par les gels.

La caractérisation de la surface des microcapsules :
La composition chimique de la surface de la microcapsule a été déterminée en utilisant trois techniques distinctes, chacune ayant une profondeur d'analyse différente : 0,2 - 3 μm pour ATR-FTIR, 20-100 Å pour XPS, et < 1 nm pour ToF-SIMS. La composition chimique de chacune des composantes de la microcapsule (c.-à-d. le noyau de gel, la PLL, et l'alginate) a été également déterminée pour aider à identifier les substances qui ont été exposées à la surface. Les études de la microcapsule ont été limitées à l'utilisation de l'alginate purifié commercialement parce que, selon des études préliminaires, il contient le moins d'impureté et possède les propriétés les plus reproductibles.

Un résumé des résultats

La détection, l'identification, et la quantification des contaminants

La mesure des contaminants communs :
Des traces de protéines, d'endotoxines, et de polyphénols ont été détectées dans tous les alginates. Leurs concentrations dans les alginates purifiés sont résumées dans le Tableau 1.

Tableau 1: Les concentrations de contaminants communs dans les alginates purifiés.

Le type de contaminant	La concentration mesurée dans l'alginate aqueuse (1% w/v)	La concentration estimée dans l'alginate sec
Les protéines	29 – 64 µg/ml	< 0,64% w/w
Les endotoxines	0.08 – 76 EU/ml	< 0,00008% w/w
Les polyphénols	0.5 – 2.4 AU	< 1% w/w

La détection des groupements chimiques étrangers avec le ATR-FTIR :

Si des contaminants étaient présents dans les échantillons, alors ils étaient indétectables au FTIR. Puisqu'il a été estimé que la concentration totale de protéines, d'endotoxines, et de polyphénols est < 1,2% w/w, il est plausible que la quantité d'impuretés ait été trop petite pour être détectée par cette technique.

La détection des éléments étrangers avec XPS (survol) :

En terme de pourcentage atomique, tous les échantillons sont composés d'environ 50% de carbone, 40% d'oxygène, et 9% de sodium. Une comparaison avec la composition théorique de l'alginate a indiqué que les échantillons contenaient un excès de carbone et de sodium. En outre, tous les alginates purifiés contenaient des traces d'éléments étrangers, y compris le soufre (0,3 – 0,7%), le phosphore (0,02 – 0,12%), et l'azote (0,2 - 1,2%). Le soufre provenait probablement des fucoidans (des polysaccharides sulfatés qui existent dans les algues), le phosphore a été attribué aux groupements phosphate des endotoxines, et l'azote a été attribué aux groupements amine des protéines. Au total, le pourcentage atomique des éléments impurs dans un alginate purifié n'était jamais > 2%.

La détection des groupements chimiques étrangers avec XPS (haute résolution) :

En négligeant les éléments étrangers, environ 16% de la composition atomique des échantillons a été associé aux groupements chimiques étrangers. La majorité de ces contaminants, représentant 12 – 15% de la composition, a été attribué à des gaz atmosphériques (c.-à-d. les hydrocarbures, CO_2, et H_2O) qui se sont adsorbés sur la surface de l'échantillon. De plus, environ 2% de la composition ont été associés aux groupements COOH. Il a été déduit que ceci provenaient des protéines et/ou des parties

insuffisamment neutralisées de la molécule d'alginate. Finalement, une impureté à base de sodium a représenté 1 - 5% de la composition, mais elle n'a pas pu être identifiée.

La mesure des contaminants par leur effet sur la viscosité :

En général, les niveaux de contamination des alginates sont corrélés avec une diminution de la viscosité de leurs solutions. En particulier, la présence des protéines, des endotoxines, et des groupements COOH, a coïncidé avec des viscosités inférieures. L'explication pour cet effet est que les contaminants ont abaissé le volume hydrodynamique des molécules d'alginate en limitant leur capacité de s'étendre. Ceci implique que les contaminants ont changé la conformation naturelle des molécules, en favorisant leurs liaisons intramoléculaires et empêchant leur interaction avec le solvant.

La mesure des contaminants par leur effet sur le comportement thermique :

En général, les niveaux de contamination des alginates sont corrélés avec une augmentation de la température de transition vitreuse. C'est-à-dire, les contaminants ont été associés à la diminution de la mobilité des molécules d'alginate. Spécifiquement, les protéines, les endotoxines, et les polyphénols, en plus des groupements COOH, sont tous corrélés avec une mobilité réduite de l'alginate. Ceci implique que les impuretés se sont liées aux molécules d'alginate d'une manière qui a modifié leurs conformations naturelles.

La mesure des contaminants par leur effet sur l'hydrophilicité :

En général, la présence des contaminants dans les alginates est corrélée avec une diminution de l'hydrophilicité de l'échantillon. En particulier, la présence des protéines, des polyphénols, de groupements COOH, et à un moindre degré, de soufre, présentait une corrélation avec l'angle de contact. Ceci implique que les contaminants ont empêché l'interaction entre les groupements hydrophiles de l'alginate (c.-à-d. les groupements COO^- et C-OH) et les molécules d'eau en se liant directement avec ces groupements et/ou en modifiant la conformation de la molécule de sorte que ces groupements aient été cachés.

L'évaluation de la bioréactivité *in vivo* des contaminants

L'évaluation de l'attraction des cellules immunitaires :

Les niveaux de contamination des alginates sont négativement corrélés avec le nombre de cellules immunitaires qui flottaient dans le liquide péritonéal après l'implantation. Ceci implique que les alginates contaminés ont stimulé les cellules immunitaires d'adhérer à la surface des billes au lieu de rester flottants. Les protéines, les endotoxines, et les groupements COOH ont semblé avoir un effet sur le nombre de cellules flottantes.

L'évaluation de la réaction péricapsulaire :

Les niveaux de contamination des alginates sont corrélés positivement avec la gravité de la réaction péricapsulaire contre des billes implantées. Spécifiquement, les protéines, les endotoxines, les polyphénols, les groupements COOH, et même l'impureté sulfatée, ont tous eu un effet observable sur la réaction. En plus, les alginates les plus hydrophiles ont eu tendance à induire des réactions moins graves. Il est plausible que les protéines qui favorisent l'adhérence des cellules immunitaires aient été adsorbées en plus grande quantité sur les surfaces hydrophobes des billes contaminées. Autrement dit, il est possible que l'adsorption non spécifique des protéines ait été empêchée par la formation d'une couche protectrice d'eau.

L'évaluation de l'adhésion des cellules immunitaires :

Les niveaux de contamination des alginates sont corrélés positivement avec le nombre de cellules immunitaires qui ont été adhérées sur les surfaces des billes implantées. Les polyphénols et les groupements COOH étaient le plus fortement associés à l'accumulation des cellules adhérées, mais les contenus de protéine, d'endotoxine, et de soufre ont aussi semblé influencer la réaction.

La caractérisation de la surface des microcapsules

La détermination de la composition chimique par ATR-FTIR :

Les spectres de FTIR ont indiqué que la partie extérieure des microcapsules (< 3 μm) était principalement composée d'alginate et de PLL. Un déplacement des bandes d'absorption qui correspondent aux groupements COO^- de l'alginate a reflété que, à l'intérieur de la membrane, des ions de sodium ont été probablement remplacés par les groupements NH_3^+ de la PLL et/ou les ions Ca^{2+} du noyau de gel. D'autres déplacements de bandes ont indiqué que la force des liaisons C-O et C-C été légèrement modifiée, probablement dus aux changements conformationels de l'alginate. L'intensité et le placement des bandes amides ont indiqué que la PLL, comme composante de la microcapsule, était principalement dans les conformations hélice-α et aléatoire, et à un moindre degré, dans la conformation feuillet-β.

La détermination de la composition chimique par XPS :

Les spectres de XPS ont indiqué que l'alginate et la PLL ont été tous les deux présents dans la partie externe des microcapsules (< 100 Å). En comparant les rapports de C/O, de C/N, et de C/Na pour les microcapsules et pour chacune des composantes, il a été estimé que 81% des atomes de carbone détectés appartenaient à la PLL tandis que 16% du carbone appartenaient à l'alginate. Un examen des spectres à haute résolution a confirmé qu'au moins 55% des atomes de carbone, 30% des atomes d'oxygène, et presque tous les atomes d'azote à la surface des microcapsules provenaient des molécules de PLL.

La détermination de la composition chimique par ToF-SIMS :

Une analyse des spectres de masse obtenus par le TOF-SIMS a démontré que l'alginate et la PLL étaient tous les deux présents dans la monocouche extérieure des microcapsules (< 1 nm). De grands fragments de la molécule d'alginate ont été pulvérisés de la surface des microcapsules tandis que les fragments de PLL avaient une tendance à être plus petits. En outre, un certain nombre d'ions lourds qui sont principalement composés de C, O, H, Na, et N ont été pulvérisés de la surface. Ces ions provenaient probablement des

complexes d'alginate-PLL qui ont été formés pendant la fabrication de la microcapsule. Des images reconstruites de la région de l'analyse ont démontré que les substances ont été homogènement distribuées à la surface. Donc, la possibilité que la PLL a été exposée à la surface à cause de ruptures dans la couche externe d'alginate a été rejetée.

Les conclusions

Les conclusions expérimentales :

Les alginates contenaient des contaminants qui ne pourraient pas être complètement éliminés par les processus chimiques. Les contaminants résiduels incluent les protéines, les endotoxines, et les polyphénols, aussi bien que le soufre, le sodium, et des groupements COOH. Après la purification, jusqu'à 7% de la composition atomique de l'alginate a pu être attribué aux contaminants de volume.

Les contaminants ont contribué à l'immunogénicité des gels d'alginate. En particulier, la présence des groupements COOH, des protéines, des polyphénols, et, à un moindre degré, des endotoxines a favorisé la réaction péricapsulaire. L'évidence a suggéré que, en plus d'être immunogènes, les contaminants ont contribué à l'induction des réactions immunitaires en modifiant la conformation et l'hydrophilicité naturelles de l'alginate pour le rendre moins biocompatible.

La monocouche extérieure des microcapsules est composée de molécules et/ou de fragments d'alginate et de PLL. Des deux, la PLL a contribué à > 50% du carbone dans la partie extérieure (< 100 Å) des microcapsules. Il a été confirmé que la PLL a été principalement liée à l'alginate pour former un complexe d'alginate-PLL. Ceci a impliqué des liaisons ioniques entre les groupements NH_3^+ et COO^-, aussi bien que deux à trois conformations différentes de la PLL (hélice-α, aléatoire, et feuillet-β). Cependent, il est possible qu'une portion de l'alginate qui a retenu le sodium n'ait pas été liée à la PLL. Finalement, l'exposition de la PLL n'était pas causé par des ruptures de la couche d'alginate.

Les contributions originales au domaine :

Ce projet a prouvé pour la première fois que, en plus d'être contaminé par des protéines, des endotoxines, et des polyphénols, les alginates contiennent des impuretés précédemment non détectées. Ce projet a également fourni la première démonstration claire que la purification chimique n'enlève pas toutes ces impuretés, et que les contaminants résiduels ont un effet profond sur la biocompatibilité des alginates. En outre, il a été démontré que les contaminants peuvent modifier la conformation et l'hydrophilicité des molécules d'alginate. Ceci a mené à l'hypothèse originale que, en plus d'être immunogènes, les contaminants sont capables d'induire indirectement une réaction immunitaire en réduisant la biocompatibilité naturelle des alginates. Aussi, c'est la première fois que la composition chimique de la monocouche extérieure des microcapsules a été directement étudiée, et ainsi, ce projet a fourni la première preuve physique de l'exposition de PLL à la surface des microcapsules.

Des recommendations pour l'avenir :

Basé sur les nouvelles évidences, il est recommandé que la biocompatibilité des alginates soit optimisée en utilisant deux approches : La première approche est d'éliminer complètement les impuretés dans les alginates. Si ceci est essayé, alors il est suggéré que des techniques physico-chimiques soient employées pour évaluer la pureté des alginates. La deuxième approche est de neutraliser les effets que les contaminants ont sur les propriétés de l'alginate. Si l'immunogénicité de l'alginate est principalement causé par des modifications de sa conformation et son hydrophilicité, alors il n'est pas nécessaire d'éliminer 100% des contaminants. Un traitement de plasma, par exemple, peut être employé pour augmenter l'hydrophilicité des alginates pour les rendre biocompatibles.

Basé sur les nouvelles preuves de la présence de PLL à la surface de la microcapsule, il est recommandé, d'une manière justifiable, que les efforts de mieux couvrir la PLL soient continués. Puisque l'exposition de la PLL ne semble pas être due aux défauts, il est suggéré que l'épaisseur de la couche externe d'alginate soit augmentée. Ceci pourrait être réalisé en augmentant la concentration d'alginate ou en réticulant les alginates avec des

ions pour former une couche épaisse de gel. En outre, il est recommandé que la surface des nouveaux designs de microcapsules soient examinées en utilisant des techniques telles que XPS et ToF-SIMS, avant de les implanter dans des animaux, car cette approche serait la plus éthique et économique.

TABLE OF CONTENTS

ACKNOWLEDGEMENTS iv

ABSTRACT v

CONDENSÉ EN FRANÇAIS ix

TABLE OF CONTENTS xx

LIST OF TABLES xxiv

LIST OF FIGURES xxvi

LIST OF APPENDICES xxviii

LIST OF ABBREVIATIONS AND ACRONYMS xxix

CHAPTER 1: INTRODUCTION 1

CHAPTER 2: REVIEW OF IDDM AND ITS TREATMENTS 3

2.1. Description of IDDM 3

2.2. Treatments for IDDM 3

2.2.1. *Injection therapy* 3

2.2.2. *Whole pancreas transplantation* 4

2.2.3. *Islet cell transplantation* 4

CHAPTER 3: REVIEW OF MICROENCAPSULATION FOR IMMUNOPROTECTION 6

3.1. The concept of immunoprotection 6

3.2. Structure of APA microcapsules 7

3.3. Properties of the microcapsule components 7

3.3.1. *Alginates* 7

3.3.2. *Alginate gels* 9

3.3.3. *Poly-L-lysine* 9

CHAPTER 4: STATE OF THE ART IN MICROENCAPSULATION 11

4.1. Induction of normoglycemia using microencapsulated islets 11

4.2. Biocompatibility of APA microcapsules 12
4.2.1. *Alginate biocompatibility* 12
4.2.2. *Exposure of PLL* 13
CHAPTER 5: RESEARCH PROBLEM 15
5.1. Statement of the problem 15
5.2. Evidence of the stated problem 15
5.3. Importance of solving the stated problem 16
CHAPTER 6: RESEARCH OBJECTIVES 17
6.1. General objective 17
6.2. Specific objectives 17
6.3. Rationale 17
CHAPTER 7: MATERIALS and METHODS 19
7.1. Design of study 19
7.1.1. *Selection of purified alginates* 19
7.1.2. *Detection, identification, and quantification of the contaminants* 19
7.1.3. *Evaluation of the in vivo bioreactivity of the alginates* 19
7.1.4. *Characterization of microcapsule surface* 20
7.1.5. *Division of responsibilities* 20
7.2. Alginate purchase and preparation 21
7.2.1. *Purchase* 21
7.2.2. *Purification* 21
7.3. Bead and microcapsule formation 22
7.4. Measurement of common contaminants in alginates 23
7.4.1. *Protein content by micro-BCA assay* 23
7.4.2. *Endotoxin content by LAL assay* 23
7.4.3. *Polyphenol content by fluorescence spectroscopy* 24
7.5. Direct detection of contaminants in alginates 24
7.5.1. *Chemical and molecular composition by ATR-FTIR* 24
7.5.2. *Elemental and chemical composition by XPS* 25

7.6. Indirect detection of contaminants in alginates 26
7.6.1. *Viscosity measurements* 26
7.6.2. *Thermal profile by DSC* 26
7.6.3. *Contact angle measurements* 26
7.7. Physicochemical analyses of APA microcapsule surface 27
7.7.1. *Chemical and molecular composition by ATR-FTIR* 27
7.7.2. *Elemental and chemical composition by XPS* 28
7.7.3. *Chemical composition and imaging by ToF-SIMS* 28
7.8. *In vivo* performance 28
7.8.1. *Implantation of barium alginate gel beads* 28
7.8.2. *Assessment of immune cell attraction* 29
7.8.3. *Assessment of induced pericapsular reaction* 29
7.8.4. *Assessment of immune cell adhesion* 29
7.9. Statistical analyses 29

CHAPTER 8: RESULTS AND DISCUSSION 30
8.1. Detection and quantification of common contaminants 30
8.1.1. *Protein content* 30
8.1.2. *Endotoxin content* 30
8.1.3. *Polyphenol content* 31
8.2. Direct detection and identification of contaminants 33
8.2.1. *Detection of foreign chemical groups by ATR-FTIR* 33
8.2.2. *Identification of foreign elements by XPS in survey mode* 35
8.2.3. *Identification of foreign chemical groups by XPS in high resolution mode* 38
8.3. Indirect detection of contaminants 42
8.3.1. *Effect on solution viscosity* 42
8.3.2. *Effect on thermal behaviour* 44
8.3.3. *Effect on wettability* 46
8.4. *In vivo* evaluations of alginate bioreactivity 48

8.4.1. *Free-floating immune cells* 48
8.4.2. *Pericapsular reaction* 50
8.4.3. *Adhered Immune Cells* 52
8.5. Chemical composition of the microcapsule surface 54
8.5.1. *FTIR measurements* 54
8.5.2. *XPS measurements* 58
8.5.3. *ToF-SIMS analysis* 62
CHAPTER 9: CONCLUDING REMARKS 67
9.1. Experimental conclusions 67
9.1.1. *Alginate contamination* 67
9.1.2. *Effect of contaminants on biocompatibility* 67
9.1.3. *Chemical composition of the microcapsule surface* 68
9.2. Limitations of this research project 68
9.3. Summary of original contributions 69
9.4. Recommendations for future research 70
REFERENCES 72
APPENDICES 78

LIST OF TABLES

Table 7.1: Summary and comparison of the protocols used for chemical purification of sodium alginates. 22

Table 8.1: Identification of peaks in the FTIR spectra of sodium alginate films. 34

Table 8.2: Elemental compositions of sodium alginate films as measured by XPS (survey scan)..... 37

Table 8.3: Chemical groups at the surface of sodium alginate films as detected by XPS (high resolution scan). 40

Table 8.4: Chemical composition of sodium alginate films as measured by XPS (high resolution scan).. 40

Table 8.5: Correlation between various properties of sodium alginate and the number of free-floating immune cells that were found 2 and 14 days after bead implantation. 49

Table 8.6: Correlation between various properties of sodium alginate and the severity of the pericapsular reaction that was evaluated 2 and 14 days after bead implantation. 51

Table 8.7: Correlation between various properties of sodium alginate and the number of immune cells that were adhered to the bead surfaces 2 days after bead implantation..... 53

Table 8.8: Assignment of FTIR absorbance bands for APA microcapsules, sodium alginate films, poly-L-lysine films, and calcium alginate gel beads. 57

Table 8.9: Surface elemental compositions of APA microcapsules and their components, as measured by XPS (survey scan).. 60

Table 8.10: Identification of positive ions that were sputtered from the surface of an APA microcapsule. 65

LIST OF FIGURES

Figure 3.1: An illustration of the concept of immunoprotection - Islet cells are enclosed in an APA microcapsule. 6

Figure 3.2: Chemical structure of a sodium alginate fragment (..GGMM..). 8

Figure 3.3: Illustration of the "egg-box" model for alginate gelation. 8

Figure 3.4: Chemical structure of poly-L-lysine hydrobromide. 10

Figure 8.1: Measured concentrations of proteins, endotoxins, and polyphenol-like compounds in alginate solutions (1% w/v).. 32

Figure 8.2: Comparison of the ATR-FTIR spectra of sodium alginate films. 34

Figure 8.3: The relative contents of carbon, oxygen, and sodium in alginate films. 41

Figure 8.4: Measured dynamic viscosity of sodium alginate solutions (2% w/v) 43

Figure 8.5: Glass transition temperature of sodium alginates as measured by DSC. 45

Figure 8.6: Measured contact angles of water on sodium alginate films 10s after contact. 47

Figure 8.7: Number of immune cells that were free-floating in the peritoneal liquid of mice after barium alginate beads were implanted into their peritoneal cavities. 49

Figure 8.8: Severity of the pericapsular reaction around barium alginate beads that were retrieved 2 days and 14 days after implantation in the peritoneal cavity of mice. 51

Figure 8.9: Number of immune cells that were adhered to the surfaces of barium alginate beads after 2 days and 14 days implantation in the peritoneal cavity of mice. 53

Figure 8.10: ATR-FTIR spectra of dehydrated APA microcapsules, sodium alginate film, dehydrated calcium alginate gel beads, and poly-L-lysine film. 56

Figure 8.11: Comparison of the elemental composition of APA microcapsules with their components, as calculated by XPS (survey scan), and in terms of the C/O ratio, C/Na ratio, and C/N ratio. 61

Figure 8.12: Positive ion mass spectra of the APA microcapsule surface, alginate film, and PLL film, as measured by ToF-SIMS. 64

Figure 8.13: Images of a 50 μm × 50 μm area of the microcapsule surface, as reconstructed from the ion mass spectra measured by ToF-SIMS. 66

LIST OF APPENDICES

Appendix A: Commercial production of alginate 78

Appendix B: Specification sheet for Pronova™ UP LVG alginate 79

Appendix C: Viscosities of alginate solutions 80

Appendix D: Penetration depth of ATR-FTIR 81

LIST OF ABBREVIATIONS AND ACRONYMS

APA	Alginate-Poly-L-lysine-Alginate
ATR	Attenuated Total Reflectance
BCA	Bicinchoninic Acid
CLSM	Confocal Laser Scanning Microscopy
CRGB	Centre de Recherche Guy-Bernier
Crude	Unpurified alginate
DSC	Differential Scanning Calorimetry
FTIR	Fourier Transform Infrared Spectroscopy
G	Guluronic acid residue
GRBB	Groupe de Recherche en Biomécanique/Biomatériaux
IDDM	Insulin-dependent Diabetes Mellitus
LAL	*Limulus* Amoebocyte lysate
M	Mannuronic acid residue
PLL	Poly-L-lysine
Pronova	Commercially purified alginate
PurKm	Alginate purified using methods described by Klock et al
PurDV	Alginate purified using methods described by De Vos et al
PurWm	Alginate purified using methods described by Prokop and Wang
ToF-SIMS	Time-of-Flight Secondary Ion Mass Spectrometry
XPS	X-Ray Photoelectron Spectroscopy

CHAPTER 1: INTRODUCTION

The only treatment for insulin-dependent diabetes mellitus (IDDM) that can induce constant normoglycemia and insulin independence is the transplantation of a pancreas or of pancreatic cells. While whole pancreas transplantation is a high-risk procedure, islet cell transplantation is potentially a much safer and accessible treatment for IDDM.

By encapsulating the islet cells within a semi-permeable membrane, they can be protected from the immune system without the use of dangerous immunosuppressive medications. This approach to preventing graft rejection is referred to as microencapsulation.

The microencapsulation technique is still in its stages of development, and its effectiveness as a treatment for IDDM in the absence of immunosuppression has not yet been clinically tested. Progress has mainly been hindered because the implanted microcapsules tend to induce a fibrotic overgrowth that leads to graft failure.

The precise causes for this immune reaction have not yet been identified. A general inability to consistently achieve microcapsule biocompatibility is proof of this fact. This is partially a consequence of insufficient information about the physicochemical details of the biomaterials.

This research project aimed to provide some explanations for the foreign body reactions in terms of the physicochemical properties of the biomaterials. In particular, various physicochemical analyses were used to search for potentially immunogenic substances in the biomaterials and at the microcapsule surface. Such an extensive investigation of the physicochemical details of microcapsules and their components has never been performed before this project.

During the course of this project, it was discovered that the biomaterials contained a number of impurities that adversely influenced their *in vivo* biocompatibility. Before, it

was generally believed that these contaminants could be removed via chemical purification, but the results of this project proved otherwise. It was also proven for the first time that an immunogenic polypeptide, which is used as a middle layer in the microcapsules, is actually exposed at the microcapsule surface.

This new evidence that potentially immunogenic substances are present in the biomaterials and at the microcapsule surface can be used to guide future modifications of the microcapsule design that aim to improve its biocompatibility. This rational, step-wise approach is critical to the success of the microencapsulation technique.

CHAPTER 2: REVIEW OF IDDM AND ITS TREATMENTS

2.1. Description of IDDM

Insulin-dependent diabetes mellitus (IDDM) is the result of an autoimmune destruction of the β-cells (American Diabetes Association 2004). β-cells are one of the cell types that make up the endocrine portions of the pancreas, a.k.a. the islets of Langerhans. These islet cells secrete insulin in response to changes in the concentration of blood glucose. Insulin is required to maintain normal levels of blood glucose by suppressing the production of hepatic glucose and by increasing the uptake and use of glucose by the muscles. The main consequence of insufficient insulin is hyperglycemia, i.e. high levels of blood glucose. If IDDM is left untreated, ketoacidosis will develop and eventually lead to coma or death.

2.2. Treatments for IDDM

2.2.1. Injection therapy

The most common treatment for IDDM requires multiple daily injections of exogenous insulin coupled with close monitoring of the blood glucose levels. While this method significantly extends the life expectancy of diabetics, it does not reproduce the natural secretory functions of normal β-cells closely enough to achieve constant normoglycemia (i.e. healthy blood glucose levels) (Calafiore 2002). Consequently, this therapy does not eliminate the risks of developing the long-term health complications that are associated with prolonged hyperglycemia, such as retinopathy, nephropathy, and neuropathy. Additionally, injection therapy is very expensive for healthcare systems, requires a strict regime that lowers the quality of life, and often induces severe and frequent hypoglycemia.

2.2.2. *Whole pancreas transplantation*

The other treatment for IDDM, which has routinely been applied for the past 15 years (Manske 1999), is the transplantation of a whole pancreas. In this case, the transplant supplies the patient with an endogenous source of insulin that can respond immediately to changes in glucose concentrations. Consequently, the patient can be independent from injections and, more importantly, constant normoglycemia can be maintained. In spite of these advantages, pancreatic transplantation is associated with significant morbidity and mortality rates. Moreover, to prevent graft rejection, patients are required to take immunosuppressive medications for the rest of their lives. These controversial medications suppress the immune system in a non-specific manner, which can lead to various health complications, and they may induce additional side effects such as kidney failure (Morris 1996). Because of these significant risks, this procedure is restricted to diabetics that have or need a kidney transplant, or have extreme difficulty with glucose control. This means that, by the time the surgery is justifiable, the patient's health complications are usually advanced and irreversible.

2.2.3. *Islet cell transplantation*

There is an alternative method to supplying endogenous insulin, which is to transplant only the islet cells of the pancreas. Islet cell transplantation, however, is still in its earlier stages of development, with only 615 islet allotransplants reported worldwide between 1990 and June 2003 (Bretzel et al. 2004). Still, the recent success of the 'Edmonton Protocol' (Shapiro et al. 2000), which had a reported 100% graft survival rate and 80% insulin independence rate, demonstrates the feasibility of islet transplantation as a therapy for IDDM. Moreover, when compared to whole pancreas transplantation, this method offers many important advantages:

- Because the islets represent only 1-2% of the total pancreatic mass, they can be transplanted by injection or minimally invasive surgery

- Islet cells can potentially be supplied by various sources other than cadaveric donors, including xenografts, engineered β-cell lines, or differentiated stem cells, thus tissue shortage can be avoided
- Though susceptible to the same graft rejection as a whole pancreas transplants, transplanted islets cells can be immunoprotected by encapsulation (refer to section 3), thus the necessity for life-long immunosuppression can be eliminated

Islet cell transplantation could therefore be the safer and more accessible method for β-cell replacement. This means that the procedure could be justified at the onset of the disease so that the development of health complications can be prevented altogether.

CHAPTER 3: REVIEW OF MICROENCAPSULATION FOR IMMUNOPROTECTION

3.1. The concept of immunoprotection

The purpose of immunoprotection is to prevent the graft rejection of transplanted islet cells without using immunosuppressive medications. It is important to avoid these medications because their use can lead to dangerous side effects and various health complications associated with non-specific suppression of the immune system (Morris 1996). In addition, the medications can have adverse effects on the grafted islet cells.

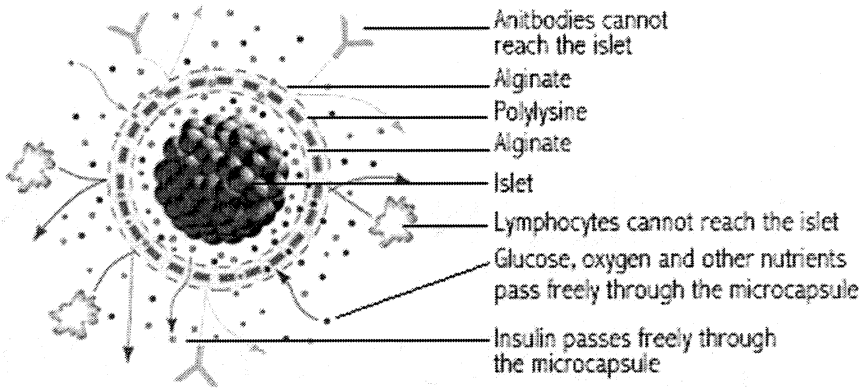


Figure 3.1: An illustration of the concept of immunoprotection - Islet cells are enclosed in an APA microcapsule. Figure is reproduced from (The Islet Foundation 2004).

The concept of immunoprotection consists of preventing immune cells and antibodies from coming into physical contact with the transplanted cells while, at the same time, maintaining cell viability and functionality. In theory, this is achieved by enclosing the cells within a semi-permeable membrane of selective porosity, filtration, and permeability (Calafiore 2002). Ideally, the membrane's molecular weight cut-off permits the free diffusion of smaller molecules (i.e. insulin, glucose, cell nutrients, and waste products) that is necessary for graft survival and function, yet blocks out larger host

molecules that facilitate the immune destruction of the implant. Figure 3.1 illustrates how islet cells can be immunoprotected by an APA microcapsule.

3.2. Structure of APA microcapsules

The Alginate-Poly-L-Lysine-Alginate (APA) microcapsule, which is illustrated in Figure 3.1, is the microcapsule type that is most frequently used for the immunoprotection of islet cells. There are three main components of the APA microcapsule:

- *Calcium alginate gel*: The gel makes up the core of the microcapsule. It serves to immobilize the islet cells.
- *Poly-L-lysine (PLL)*: A layer of PLL surrounds the gel core. This layer bonds electrostatically to the core alginate to form the semi-permeable membrane that serves to immunoprotect the enclosed cells. The addition of PLL also improves the stability of the microcapsule.
- *Alginate*: The microcapsule is coated with an outer layer of alginate. This coating serves to bind the positive charges of the PLL. Unbound PLL must be covered with a biocompatible layer because it can be immunogenic (Strand et al. 2001).

3.3. Properties of the microcapsule components

3.3.1. Alginates

Alginates are salts of alginic acid. Structurally, alginic acid is a linear copolymer composed of 1-4-linked β-D-mannuronic (M) and α-L-guluronic acid (G) (Ertesvag and Valla 1998, Smidsrod and Skjak-Braek 1990). The monomers can be arranged in blocks of consecutive G-residues (GG blocks), consecutive M-residues (MM blocks), or alternating M and G residues (MG blocks). The relative amount of each block type in the alginate depends on the species and tissue they are isolated from. The chemical structure of the sodium salt of alginic acid, i.e. sodium alginate, is illustrated in Figure 3.2.

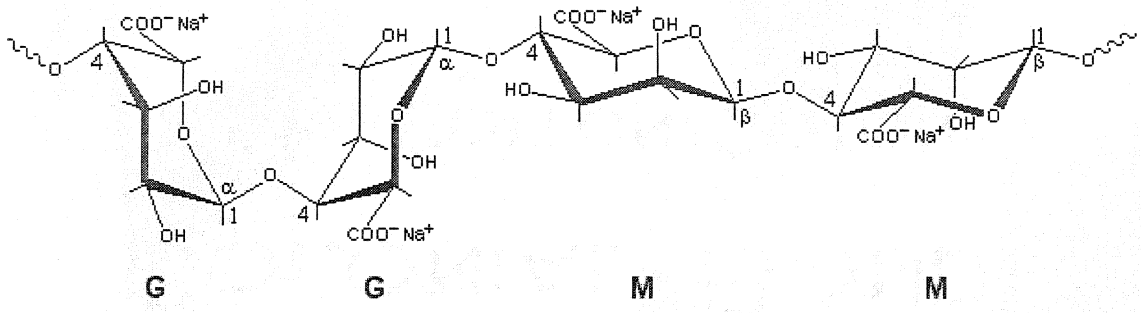


Figure 3.2: Chemical structure of a sodium alginate fragment (..GGMM..). G: Guluronic acid residue; M: Mannuronic acid residue. Adapted from a figure in (Chaplin 2004).

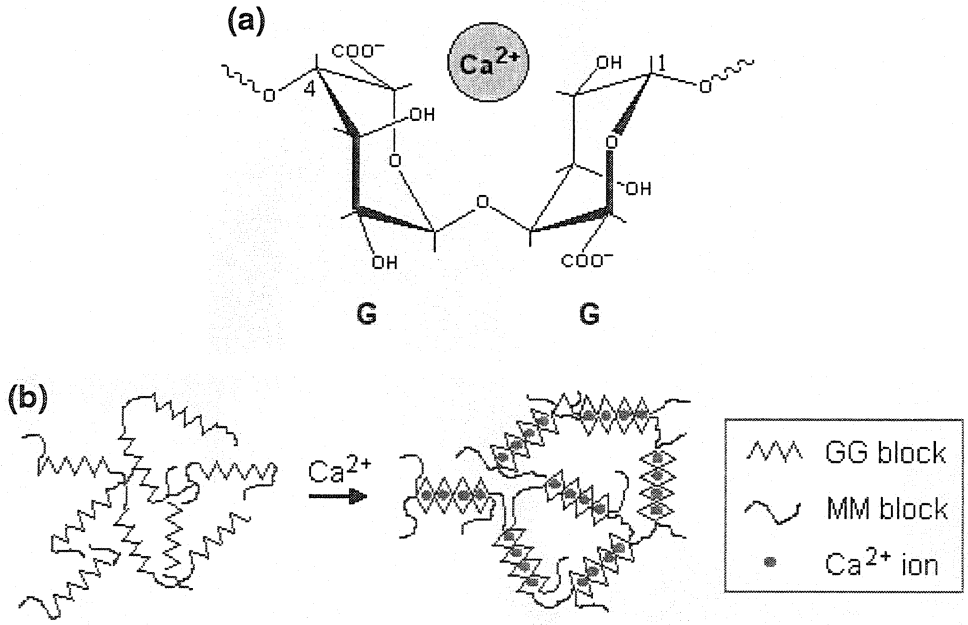


Figure 3.3: Illustration of the "egg-box" model for alginate gelation. This figure shows **(a)** the binding site of a Ca^{2+} ion between two G residues, and **(b)** the cross-linking of several GG blocks by the addition of Ca^{2+} ions. Based on a figure in (Smidsrod and Skjak-Braek 1990).

Alginates are the major constituents of the cell walls in brown algae, a.k.a. *Phaeophyta*. To produce commercial alginates, the salts must first be extracted from the seaweed, converted to alginic acid, and then re-neutralized to produce the desired salt or alginate (FMC BioPolymer 2004). The entire process, which can require over 20 stages, is summarized in Appendix A.

3.3.2. Alginate gels

Alginate solutions form a gel in the presence of divalent cations (Smidsrod and Skjak-Braek 1990). For the purpose of cell immobilization, Ca^{2+} and Ba^{2+} ions are most commonly used for gelation. Gel network formation principally consists of a dimerization of GG blocks that selectively bind the cations. That is, when two GG blocks are aligned, their buckled ribbon structure forms of an array of cavities that is often referred to as the "egg-box". These cavities function as binding sites for ions (the "eggs"), and bonds formed between these sites give rise to the junction zones of the gel network. This "egg-box" model for alginate gelation is illustrated in Figure 3.3.

The strength of the gels is dependant on the proportion of GG blocks in the alginate, as well as the affinity of the divalent cation (Smidsrod and Skjak-Braek 1990). Destabilization of the gel may occur in the presence of certain chelating compounds (e.g. phosphate, citrate, lactate) or cations that can replace the cross-linker ions (e.g. Na^{+}, Mg^{2+}). The stability, on the other hand, can be increased by using divalent cations with a higher affinity for alginate and/or by forming alginate-polycation complexes that do not dissolve in the presence of chelators or anti-gelling cations.

3.3.3. Poly-L-lysine

Poly-L-lysine is a positively charged chain of amino acids. The chemical structure of the hydrobromide salt of PLL is shown in Figure 3.4.

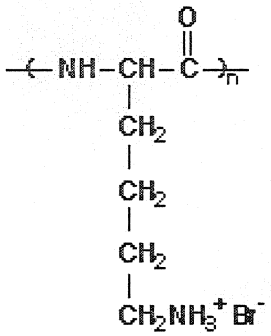


Figure 3.4: Chemical structure of poly-L-lysine hydrobromide. Adapted from a figure in (Ihara 2004).

CHAPTER 4: STATE OF THE ART IN MICROENCAPSULATION

4.1. Induction of normoglycemia using microencapsulated islets

The feasability of islet cell microencapsulation as a method to induce normoglycemia has been demonstrated on several occasions using animal models. Since the first reported success of this technique (Lim and Sun 1980), a number of research groups have used microencapsulated islet cells to reverse the diabetic state of rodents for periods lasting several months (Rayat et al. 2000, Fan et al. 1990). This technique has also induced normoglycemia that could be maintained for months in dogs (Soon-Shiong et al. 1992) and monkeys (Sun et al. 1996). However, these results using large animal models have not yet been reproduced, nor have they been followed by clinical studies.

Clinical trials of this method for treating IDDM are in their first stages of development. In the past, there has only been a single published case of insulin independence after transplantation of microencapsulated islets in an immunosuppressed human patient (Soon-Shiong et al. 1994). For the future, pilot phase-1 clinical trials of alginate/PLO microencapsulated islet grafts in non-immunosuppressed patients were reportedly approved in September 2003 (Orive et al. 2004).

Despite the proven feasibility of the treatment, researchers have difficulty maintaining the proper function of the microencapsulated islets for more than a few months and the reproducibility of the results is unsatisfactory. Graft failure is most commonly attributed to a fibrotic overgrowth that eventually surrounds the transplant and restricts the free diffusion of cell nutrients and other small molecules across the microcapsule membrane.

4.2. Biocompatibility of APA microcapsules

Several studies have demonstrated that the foreign body reactions that accompany graft failure are induced by a poor biocompatibility of the microcapsules rather than, or in addition to, the immunogenicity of the encapsulated islets (Fritschy et al. 1994, Wijsman et al. 1992). Researchers are thus aiming to identify which features of the microcapsule are contributing to its immunogenicity. Apart from individual imperfections, there are two general explanations for the adverse reactions to the microcapsules: (1) The alginate coating is not fully biocompatible, and/or (2) The immunogenic PLL is exposed at the microcapsule surface.

4.2.1. Alginate biocompatibility

For the most part, any immunogenicity that alginate has displayed has been attributed to the presence of contaminants. Specifically, proteins, endotoxins, and polyphenols are commonly detected as impurities in both freshly extracted and commercially produced alginates. Studies have shown that the removal of these contaminants decreases the mitogenicity and the *in vivo* reactivity of alginate solutions and gels (Leinfelder et al. 2003, Klock et al. 1994, Zimmermann et al. 1992). The results of i*n vivo* studies using APA microcapsules have also implied that alginate, as a microcapsule coating, has a reduced biocompatibility when it is contaminated (Orive et al. 2002, De Vos et al. 1997b).

It has been suggested that only the M residues are responsible for the mitogenic activity of alginates (Kulseng et al. 1996, Otterlei et al. 1993, Otterlei et al. 1991). A study showing that high-M microcapsules are more immunogenic than high-G microcapsules supports this view (Kulseng et al. 1999). In contrast, others have observed that high-G microcapsules induce the stronger foreign body reaction (Clayton et al. 1991). Moreover, it has been shown that, if purified, high-M alginates do not induce any mitogenic activity (Klock et al. 1997). A recent study suggested that high-M alginates are more susceptible

to contamination (Orive et al. 2002), which not only explains the disagreement between studies, but also re-emphasizes the role of impurities in alginate immunogenicity.

There have been few other suggested explanations for the alginate's immunogenicity. The origin of the alginate plays a role in its biocompatibility (Leinfelder et al. 2003), if not only because of its direct impact on the M/G ratio and the contamination level of the alginate. Additionally, in one study, higher molecular weight (M-rich) alginates were suspected to be less biocompatible (Otterlei et al. 1993). Otherwise, no published studies have been found that directly investigate the impact of other properties, such as charge and conformation, on the bioreactivity of alginate.

4.2.2. Exposure of PLL

A very common explanation for the foreign body reactions against APA microcapsules is the exposure of PLL at the surface (Clayton et al. 1991). Seeing that unbound PLL is known to be immunogenic (Strand et al. 2001), this is a reasonable hypothesis.

To support this view, the exposure of PLL has been experimentally implied: APA microcapsules were shown to induce a stronger immune response than microcapsules without a PLL layer, despite that the alginate was identical in both cases (King et al. 2001, De Vos et al. 1997a). Furthermore, it has been shown that, in the absence of the outer alginate coating, PLL may detach from the inner gel core when stored in a saline solution for several days (Thu et al. 1996).

A few recent investigations of the microcapsule membrane have indicated that the PLL may not form a distinct layer between the gel core and outer alginate coating. One group, using confocal laser scanning microscopy (CLSM), suggested that the alginate coating overlaps the PLL layer rather than forming an additional outer layer (Strand et al. 2003). Another research group discarded the simple three-layer model after performing XPS and FTIR investigations of the PLL-alginate binding (van Hoogmoed et al. 2003, de Vos et al. 2002).

Other suggested factors that contribute to the foreign body reactions against the APA microcapsules tend to relate to the issue of PLL exposure. Among these factors are the M/G ratio of the alginate and the incubation times during microcapsule formation, either of which may have an impact on both the binding of PLL to the gel core and the binding of the outer alginate coating to the PLL (Thu et al. 1996).

CHAPTER 5: RESEARCH PROBLEM

5.1. Statement of the problem

The current information about the physicochemical properties of purified alginates and APA microcapsules is not sufficient to explain the inflammatory and immune responses that are observed under *in vivo* conditions.

5.2. Evidence of the stated problem

Despite purification of the alginates, unexplainable inflammatory and immune responses to both alginate gels (Klock et al. 1997) and APA microcapsules (De Vos et al. 1997b) can be observed. Furthermore, experimental results between research groups are often conflicting and lacking in reproducibility, particularly when the *in vivo* biocompatibility of the biomaterials is concerned. These facts emphasize that the bioreactivities of alginate and APA microcapsules are still poorly understood and that some factors that influence the foreign body response have not yet been identified.

The current information about the biomaterial properties of alginates and microcapsules is deficient in two main areas:

Alginate contamination: In general, proof of alginate purity has been provided using routine assays (e.g. Bradford, LAL, and fluorescence spectroscopy) that measure their protein, endotoxin, and polyphenol contents. These assays, however, are biased, meaning that they are specific to the detection of these three contaminant types. As a consequence, it is undetermined whether alginates contain other potentially immunogenic impurities, including fucoidans and laminarans (other polysaccharides that exist in brown algae), polymer fractions, nucleotides, various heavy metals, yeast, and mould (Zimmermann et al. 1992, Skjak-Braek G. et al. 1989) that may be undetectable using standard assays.

Microcapsule surface composition: Investigations of the microcapsule exterior have been few, recent, and tended to provide ambiguous results. For instance, an examination of the membrane using CLSM could not explain variations in microcapsule biocompatibility (Strand et al. 2003), possibly due to inadequate resolution. Furthermore, the analytical depths of XPS and FTIR correspond to several monolayers, and so results of these analyses may not represent to the 'true' microcapsule surface (i.e. the outermost atomic layer). The fact is, many physicochemical details of the microcapsule surface, including the degree of PLL exposure, are still unknown.

5.3. Importance of solving the stated problem

If the information about the physicochemical properties of the alginates and microcapsules is not improved, then certain factors that are inducing the immune reaction might not be identified. As a consequence, the *in vivo* biocompatibility of microcapsules will continue to be variable and difficult to reproduce because important biomaterial properties will be inadequately controlled.

It is absolutely necessary to achieve adequate *in vivo* biocompatibility in a consistent and reproducible manner if graft survival is to be prolonged and if APA microcapsules are to be approved for clinical studies. In other words, solving the stated problem is of critical importance for the progress and success of islet cell microencapsulation as a treatment for IDDM.

CHAPTER 6: RESEARCH OBJECTIVES

6.1. General objective

The general objective of this research project was to explain the *in vivo* bioreactivity of purified alginates and APA microcapsules in terms of their physicochemical properties.

6.2. Specific objectives

The specific objectives of this project were:

(1) To identify and quantify the contaminants that are present in alginates after purification
(2) To evaluate the effect of these contaminants on the *in vivo* biocompatibility of the alginates
(3) To determine the chemical composition of the microcapsule's true surface

6.3. Rationale

There is a high probability that alginates contain impurities that are undetectable using routine analytical assays. If these impurities are contributing to the foreign body reactions against alginates, then they must be identified so that they can be eliminated. Furthermore, ensuring that there are no immunogenic impurities in the purified alginates is a prerequisite to investigating the effects of other properties, such as the M/G ratio, on the biocompatibility of the alginates and of the microcapsules.

Despite recent studies of the membrane composition, there has been no direct evidence of PLL exposure at the microcapsule surface. It is essential to determine the chemical composition of the outermost atomic layer of the microcapsule in order to verify whether

PLL, or any other immunogenic substance, is in fact exposed before large amounts of time and money are invested into the development of new microcapsule designs.

In the long term, the ability to explain the bioreactivity of the biomaterials in terms of their measurable physicochemical properties will have two important benefits. First of all, the information can be used as a guide to rationally tailor the properties of the biomaterials, via chemical or physical processes, in order to optimize their biocompatibility. Secondly, an ability to predict a microcapsule's biocompatibility from its physicochemical properties will permit new microcapsule designs to be screened before implantation. This can reduce the costs, time, and risks that are associated with *in vivo* experiments.

CHAPTER 7: MATERIALS AND METHODS

7.1. Design of study

7.1.1. Selection of purified alginates

Purified alginates were obtained by chemically treating a commercial, pharmaceutical grade alginate. To allow a comparison with the literature, three different purification protocols, each based on a published study (Klock et al. 1994) (Prokop and Wang 1997) (De Vos et al. 1997b), were applied. In addition, a commercially available alginate, which is promoted as being highly purified and of biomedical grade, was investigated. To control any effects of the M/G ratio, only high-G alginates were studied. The crude pharmaceutical grade alginate served as a control.

7.1.2. Detection, identification, and quantification of the contaminants

The alginates were tested *in vitro* for the presence of impurities that were not eliminated by, or that were introduced during, the purification process. Standard analytical techniques (fluorescence spectroscopy, LAL assay, and micro-BCA assay) were applied to measure quantities of polyphenols, endotoxins, and proteins that are commonly found in alginates. ATR-FTIR and XPS were applied to detect, qualitatively and quantitatively, the presence of all contaminating (and native) elements and chemical groups. Viscometry, DSC, and the contact angle technique were applied to detect the presence of impurities in an indirect manner by measuring their effects of the viscosity, the thermal response, and the wettability of the alginates.

7.1.3. Evaluation of the in vivo bioreactivity of the alginates

To evaluate the *in vivo* bioreactivity of the alginates, barium alginate gel beads were implanted into the peritoneal cavity of mice. Barium was chosen as a cross-linker ion

because the corresponding gels are more stable than calcium alginate gels. After 2 and 14 days implantation, the foreign body reaction induced by the beads was assessed in terms of the number of immune cells that were floating in the peritoneal liquid and in terms of the severity and fibrotic content of the pericapsular reaction. The results of the *in vivo* studies were compared to those of the *in vitro* studies in order to expose any correlations between the impurity content of the alginates and immunogenicity of the gels.

7.1.4. Characterization of microcapsule surface

The chemical composition of the microcapsule surface was determined using three separate techniques, each having a different depth of analysis: 0.2-3 μm for ATR-FTIR, 20-100 Å for XPS, and < 1 nm for ToF-SIMS. The chemical composition of each of the microcapsule components (i.e. the gel core, PLL, and alginate) was also determined in order to identify the substances that were exposed at the surface. Microcapsule studies were limited to the use of the commercially purified alginate because, according to preliminary studies, this alginate contained the least impurities and had the most reproducible properties when compared to the other alginates.

7.1.5. Division of responsibilities

Due to the multidisciplinary nature of this study, it was designed as a collaboration project between two research groups, the Centre de Recherche Guy-Bernier (CRGB) of the Maisonneuve-Rosemont Hospital and the Groupe de Recherche en Biomécanique/Biomatériaux (GRBB) of the École Polytechnique. Because the CRGB is oriented towards biological studies and biochemistry while the GRBB specializes in biomaterial characterization and physicochemistry, the experimental work was divided accordingly between the two groups. Specifically, Julie Dusseault, a Ph.D. student at the Université de Montréal and member of the CRGB, was responsible for the chemical purification of the alginate, the standard assays for the measurement of common contaminants, the viscosity measurements, and all of the *in vivo* studies; the author of this thesis report, a M.A.Sc. student at the École Polytechnique and member of the GRBB,

was responsible for all of the *in vitro* physicochemical analyses of the alginates and the characterization of the microcapsule surface.

7.2. Alginate purchase and preparation

7.2.1. Purchase

Two commercial high-G sodium alginates, Protanal® LF 10/60 and Pronova™ UP LVG, were purchased (FMC Biopolymer). Protanal® LF 10/60 is a pharmaceutical grade alginate with a 65 – 75% G content (as specified by the manufacturer). Pronova™ UP LVG has a 67% G content (as specified by the manufacturer), and is promoted as a highly purified alginate developed for the use in biomedical as well as pharmaceutical applications. The specification sheet for the Pronova™ UP LVG alginate can be found in Appendix B.

7.2.2. Purification

No additional purification of the Pronova™ UP LVG alginate was performed. The Protanal® LF 10/60 alginate was chemically purified using one of three different protocols that were based on methods described in published studies (Klock et al. 1994) (Prokop and Wang 1997) (De Vos et al. 1997b). These protocols for purification are summarized and compared Table 7.1. At least two batches of each chemically purified alginate were made on separate occasions, and samples from both batches were included in the analyses. Crude (i.e. unpurified) Protanal® LF 10/60 alginate served as a control.

For the presentation of the results, the abbreviation "Crude" was used to denote the unpurified alginate, "PurKm", "PurWm", and "PurDV" were used to denote the three chemically purified alginates, and "Pronova" was to denote the commercially purified alginate.

Table 7.1: Summary and comparison of the protocols used for chemical purification of sodium alginates. A × signifies the inclusion of the described purification step in the corresponding protocol.

Protocol Step	Purification Protocol		
	PurKm	PurWm	PurDV
Dissolution in EGTA			×
Filtration			×
Precipitation as alginic acid			×
Chloroform extraction	×	×	
Chloroform/butanol extraction			×
Dissolution in water	×	×	×
Carbon treatment (acid-washed)	×	×	
Carbon treatment (not acid-washed)	×	×	
Filtration	×	×	
Barium bead formation	×		
Acetic acid treatment	×		
Sodium citrate treatment	×		
Ethanol treatment	×		
Dissolution by EDTA	×		
Filtration	×		
Dialysis	×	×	
Filtration	×	×	
Precipitation	×	×	×
Lyophilisation	×	×	×

7.3. Bead and microcapsule formation

Alginates were dissolved in a 0.9% NaCl solution buffered to a pH of 7.4. The concentration of the alginate solution was adjusted to obtain a viscosity of 200 ± 20 cps (1.3 - 2.3% w/v, depending on the alginate). Previous studies showed that 200 cps was the ideal viscosity to avoid morphological defects of the microcapsules. All of the solutions were sterilized by filtration (0.2µm). For the production of alginate droplets, the solution was extruded through a 25-gauge needle using an electrostatic drop generator.

The droplets were transformed into gel beads by immersing them for 30 minutes in a solution containing divalent ions (10 mM $BaCl_2$ or 100 mM Calcium lactate). Barium alginate gel beads were rinsed and stored in a saline solution. For the formation of the microcapsule membrane, calcium alginate gel beads were successively incubated in a 0.05% PLL solution for 5 minutes, rinsed with a saline solution, incubated in a diluted (1:10) alginate solution for 5 minutes, then rinsed twice more with a saline solution. The final diameter of the beads and microcapsules were close to 250 µm and 280 µm respectively, as measured by light microscopy.

7.4. Measurement of common contaminants in alginates

For these analyses, alginates first were dissolved in sterile water, at a concentration of 1% w/v, and then sterilized by filtration (0.2µm).

7.4.1. Protein content by micro-BCA assay

The protein content of the samples measured using a commercial micro-BCA assay, following the protocol of the kit instructions. The alginate solutions were diluted with water in ratios of 1:1 to 1:10 000, and then incubated with the BCA reagent. Proteins were detected by the presence of a purple color that results from the formation of a peptide – copper ion – BCA complex. To quantify the protein concentrations in each solution, the intensity of light absorbance at 540 nm, which marks the purple colour, was measured using a spectrophotometer and then calibrated using a standard protein curve.

7.4.2. Endotoxin content by LAL assay

The endotoxin content of the samples was determined using a commercial *Limulus* Amoebocyte lysate (LAL) assay (E-Toxate®, Sigma-Aldrich, Inc.), following the protocol of the kit instructions. The alginate solutions were diluted with endotoxin-free water in ratios of 1:10 to 1:5000, and then incubated with the LAL reagent. Endotoxins

were detected by a characteristic clotting reaction, marked by an increase in viscosity and opacity of the samples. To quantify the endotoxin levels in the solutions, their augmented viscosities were measured and calibrated using a standard endotoxin curve.

7.4.3. Polyphenol content by fluorescence spectroscopy

The fluorescence spectra of the alginate solutions were obtained using a standard fluorescence spectrometer. Polyphenolic compounds were detected by the presence of a characteristic peak in the emission spectrum near 450 nm (Skjak-Braek G. et al. 1989). The relative quantity of polyphenols was determined by the measured fluorescence intensity at this wavelength.

7.5. Direct detection of contaminants in alginates

For the following physicochemical analyses, the alginates were first dissolved in sterile water (2% w/v) then sterilized by filtration (0.2μm). Because the analytical techniques require a dry sample, the solutions were cast into a film form. Alginate powders were also tested as a dry sample form, but the results proved to be very difficult to reproduce due to the significant impact of the particle size on FTIR and XPS signals. A concentration of 2% w/v was selected because it was within the concentration range that is used for microcapsule fabrication, and because films of lower concentration were brittle and difficult to handle. Pure water was used rather than a saline solution to avoid a false interpretation of the sodium content in the alginates.

7.5.1. Chemical and molecular composition by ATR-FTIR

Alginate films were cast on glass microscope slides and dried in a vacuum desiccator for at least 24 hours before analysis. Two films of each sample were peeled from the slides and pressed onto each side of a germanium ATR crystal using a metal clamp. During preliminary studies, ATR-FTIR was proven to be a more suitable technique to analyze the films than transmission FTIR. That is, transmission FTIR resulted in signal saturation

and a lack of reproducibility due to variations in the film thickness. Spectra were obtained using an Excalibur FTS 3000 FTIR Spectrometer (Digilab, Inc.). To avoid signal interference from water and CO_2 vapours in the atmosphere, the samples were analyzed in a nitrogen-purged chamber at room temperature. Spectra were recorded for the range 400-4000 cm^{-1} at a resolution of 8 cm^{-1}. Each spectrum represents an average of 256 scans. Background spectra consist of the bare Ge crystal under the same experimental conditions. Three trials were completed for each sample.

7.5.2. Elemental and chemical composition by XPS

Alginate solutions were agitated ultrasonically for 30 minutes immediately before casting them onto 1cm^2 silicon squares. Tests results proved that ultrasonic agitation is necessary to reduce the variability of the results by homogenizing the solutions. Silicon was selected as a substrate in place of glass due to its ability to reduce the charge effect (i.e. a spectral shift that is associated with insulating samples). To prevent the film from peeling under the high vacuum conditions associated with XPS (~10^{-9} Torr), the films were dried slowly under atmospheric conditions for at least 24 hours before transferring them to the desiccator for another 24 hours before analysis. XPS spectra were obtained using an Escalab MKII surface analysis system (VG Scientific). An unmonochromated Mg Kα anode operated at 216 W (18 mA, 12kV) was used for X-ray generation. Survey spectra were recorded for 0 – 1200 eV binding energy range, at a pass energy of 50 eV. High resolution spectra of C_{1s}, O_{1s}, and Na_{1s} peaks were recorded at 20 eV pass energy. To avoid sample degradation during analyses, exposure to X-ray radiation was limited by omitting high resolution scans of low intensity peaks and recording scans only once. Spectral analysis was performed using the software supplied by the company (Avantage, VG Scientific). Charge shift corrections were made by setting the C_{1s} peak of saturated hydrocarbons to 285.0 eV. Peaks were fitted by fixing the full-width half maximum of the C_{1s}, O_{1s}, and Na_{1s} peaks at 1.6 eV, 1.8 eV, and 1.7 eV, respectively, and setting the Gaussian/Lorentzian ratio to 50%. Three trials were completed for each sample.

7.6. Indirect detection of contaminants in alginates

For the following analyses, the alginates were first dissolved in sterile water (2% w/v) then sterilized by filtration (0.2μm). Because the analytical techniques (with the exception of viscometry) require a dry sample, and moreover, to keep the sample form consistent with the previously described analyses, the solutions were cast into a film form.

7.6.1. Viscosity measurements

The dynamic viscosities of the alginate solutions were measured using a Synchro-Lectric rotational viscometer (Brookfield Engineering Laboratories, Inc.). Each alginate was analyzed at solution concentrations ranging from 0.4% to 3% w/v.

7.6.2. Thermal profile by DSC

Alginate films were cast on glass microscope slides and dried in a vacuum desiccator for at least 24 hours before analysis. The films were peeled, trimmed to a weight of 9 ± 1 mg, and sealed in small aluminum crucibles. Thermal profiles of the alginates were recorded using a DSC131 differential scanning calorimeter (Setaram, Inc.). The instrument was calibrated using In, Sn, and Hg samples before analysis. To anneal the films, the samples were heated to170°C at a rate of 20°C/min, held at isotherm for 5 minutes, then cooled to 20°C. After allowing the polymers to rest overnight, the samples were heated a second time in the same manner. Using the software provided (SetSoft2000, Setaram), the glass transition temperature was measured for the second heating. Reference profiles were recorded using an empty aluminum crucible. Due to malfunctions of the instrumentation, only one trial could be completed during the research period.

7.6.3. Contact angle measurements

Alginate films were cast on glass microscope slides and dried in a vacuum desiccator for at least 24 hours before analysis. The left and right contact angles of water on the

(unpeeled) films were measured using a VCA Optima System (AST Products, Inc.). A water drop of 1.0 µl volume was deposited on the film surface using a mechanically controlled syringe, and a photograph was taken 10s after contact. For each trial, the angles were measured at three spots on each film. Four trials were completed for each sample.

7.7. Physicochemical analyses of APA microcapsule surface

For the studies of the microcapsule surface, only the commercially purified Pronova™ alginate was used for the fabrication of microcapsules and their components. This alginate was selected because of its low contamination level and reproducible characteristics relative to the other alginates. To wash off excess saline solution that could interfere with the results, microcapsules and beads were quickly rinsed three times with sterile water then placed on silicon squares. Aqueous solutions of alginate (2% w/v) and of poly-L-lysine (4% w/v) were also cast onto silicon squares. All samples were left to slowly air-dry for a minimum of 24 hours, then stored in a vacuum dessicator for at least 24 hours before analyses.

7.7.1. Chemical and molecular composition by ATR-FTIR

A Biorad UMA 250 Microscope (Digilab, Inc.) equipped with Micro-ATR (germanium ATR crystal) was used to acquire FTIR spectra. Single reflection micro-ATR was used in place of standard ATR-FTIR (as was used for the films) because the small contact area allowed an easy analysis of the tiny microcapsules and beads, and because the microscope accessory permitted a visual examination of the analyzed microcapsule surface. Spectra were recorded for the range 400-4000 cm^{-1} at a resolution of 8 cm^{-1}. Each spectrum represents an average of 256 scans. Background spectra consisted of the bare Ge crystal under the same experimental conditions. The experiments were repeated twice to verify that the spectra were consistent between individual samples.

7.7.2. Elemental and chemical composition by XPS

XPS spectra of the samples were recorded and analyzed as described in section 7.5.2. Three trials were completed for each sample.

7.7.3. Chemical composition and imaging by ToF-SIMS

ToF-SIMS data was acquired using a ToF-SIMS IV instrument (ION-TOF GmbH). High resolution ion mass spectra were obtained using a 15-keV Ga^+ ion source with a 1.35 pA beam current. Samples were analyzed at a pressure around 1.6×10^{-9} Torr. Total area spectra of the intact microcapsule surface, the alginate film, and the PLL film were recorded. A spectral analysis using the provided software was performed to identify the characteristic ions associated with peak in the mass spectrum. These ion masses were used to reconstruct an image of the analyzed area of the microcapsule surface. Due to experimental difficulties and time constraints, only preliminary trials were completed.

7.8. *In vivo* performance

All of the procedures involving animal use were reviewed by the animal care ethic committee of the CRGB and were stated to conform to the ethical guidelines of the Canadian Council for Animal Care.

7.8.1. Implantation of barium alginate gel beads

Male C57Bl/6 mice were used as implant recipients. Under anesthesia (isoflurane), 1000 barium alginate beads were injected into the peritoneal cavity of each mouse using a 16-gauge catheter. After 2 and 14 days implantation, the beads were recovered by peritoneal washing. For each alginate type, six mice were used as implant recipients.

7.8.2. Assessment of immune cell attraction

After 2 and 14 days implantation, immune cells that were free-floating in the peritoneal fluid were retrieved from the peritoneal cavity. The cells were then examined and counted using a Spotlite hemacytometer under the magnification of a light microscope.

7.8.3. Assessment of induced pericapsular reaction

The freshly recovered beads were counted using light microscopy. The severity of the induced pericapsular reaction was quantified using a scoring system. Specifically, each recovered bead was assigned one of the following scores: 0 = no cells were adhered to the bead surface, 1 = the bead surface was partially covered with adhered cells, 2 = the bead surface was completely covered with adhered cells.

7.8.4. Assessment of immune cell adhesion

The recovered beads were rinsed with a saline solution and then incubated at 37°C in a digestion solution containing 0.75% collagenase, 0.25% Dnase, and 0.25% trypsin. Every three minutes, the samples were vortexed and the state of digestion was verified. Once the adhered immune cells became unattached from the beads, the digestion was stopped by placing the samples on ice. The cells were recovered, washed using an HBSS solution containing 10% v/v newborn calf serum, and then counted using a hemacytometer.

7.9. Statistical analyses

Unless otherwise stated, results were compared using the unpaired Student's *t*-test (two-tailed, unequal variance). A difference for which $p < 0.05$ was considered statistically significant.

CHAPTER 8: RESULTS AND DISCUSSION

8.1. Detection and quantification of common contaminants

As shown in Figure 8.1, traces of proteins, endotoxins, and polyphenol-like compounds were detected in all of the purified alginates. A comparison with the control shows that these contaminants were present in the alginates before purification. Though it appears that, in a couple of cases, the purification process introduced additional contamination, this effect was not statistically significant. Indeed, the majority of the purified alginates contained significantly less amounts of contaminants than the crude alginate.

8.1.1. Protein content

As shown in Figure 8.1(a), the measured concentrations of protein in the purified alginate solutions ranged from 29 - 64 μg/ml. Given that the solution concentration was 1% w/v, it can be estimated that the dry alginates contained no more than 0.64% of their weight as protein contamination. This value is of the same order of magnitude as the concentration specified by the manufacturer, which was reported to be < 0.1% for the Pronova alginate.

8.1.2. Endotoxin content

As shown in Figure 8.1(b), the measured concentrations of endotoxins in the purified alginate solutions ranged from 0.08 - 76 EU/ml. The endotoxin concentration specified by the manufacturer, which was reported to be 16 EU/ml for the Pronova alginate, is within this range. According to the commonly used Reference Standard Endotoxin EC-6 conversion (Cooper 2003), the alginate solutions contained the equivalent of 0.008 - 7.6 ng/ml of endotoxins. For a solution concentration of 1% w/v, it can thus be estimated that the dry alginates contained no more than 0.00008% of their weight as endotoxin contamination.

8.1.3. Polyphenol content

For the purified alginate solutions, the measured fluorescence intensity at the polyphenol-related wavelength ranged from 0.5 – 2.4 AU, as shown in Figure 8.1(c). Assuming that the polyphenol concentration is linearly proportional to fluorescence intensity, the purified alginates contained 3-18% of the polyphenols measured in the crude alginate. Though a conversion to an absolute concentration was not possible due to a lack of standard for calibration, other research groups have made quantitative estimates of the polyphenol content in alginates (Skjak-Braek G. et al. 1989). They calculated that polyphenols represented < 1% w/w of the purified alginates, and < 8 – 17% of the crude alginates.

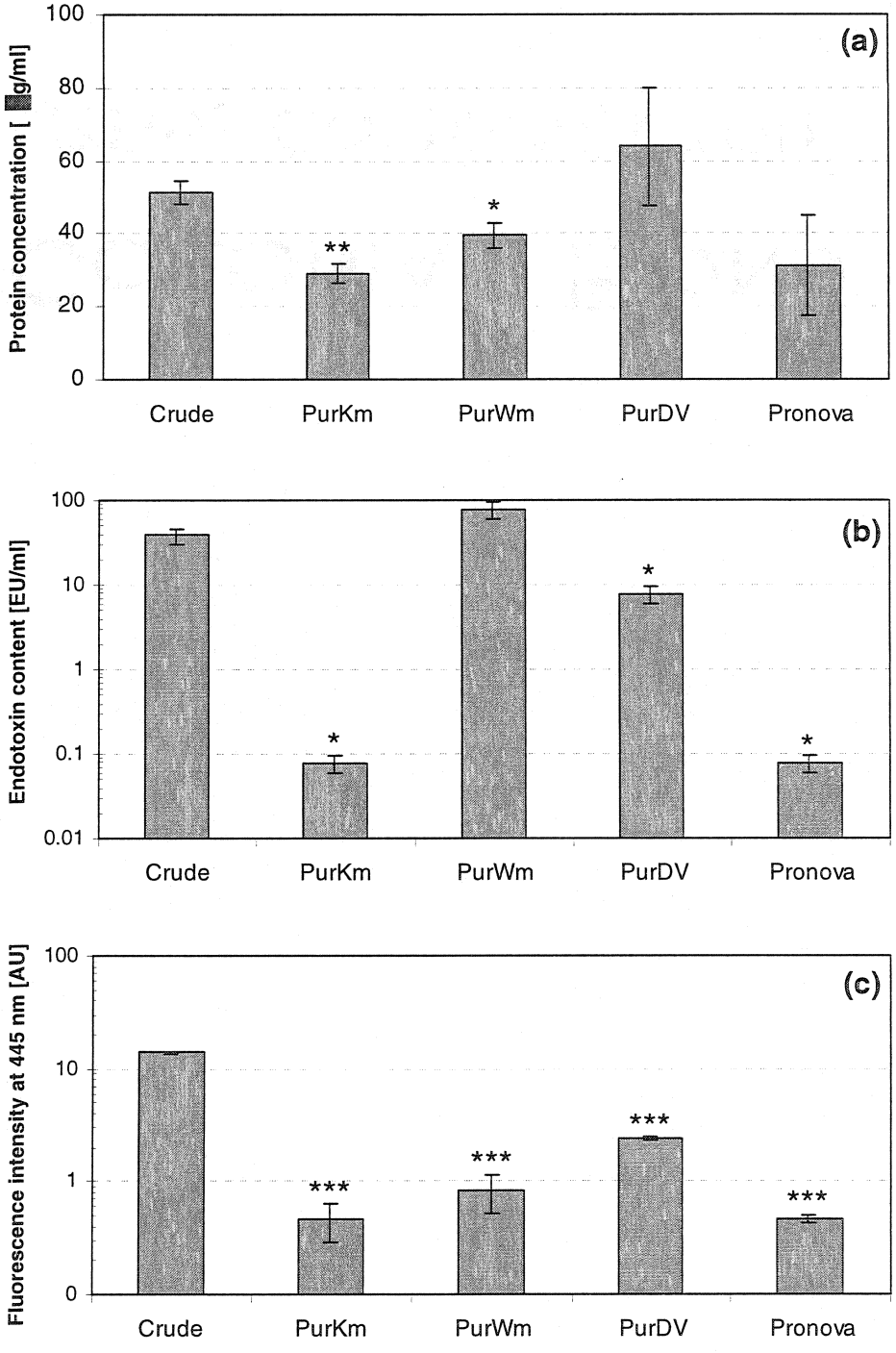


Figure 8.1: Measured concentrations of **(a)** proteins, **(b)** endotoxins, and **(c)** polyphenol-like compounds in alginate solutions (1% w/v). Results are expressed as the mean ± SEM. * $p < 0.05$, ** $p < 0.01$, *** $p < 0.001$ when compared to the crude alginate.

8.2. Direct detection and identification of contaminants

8.2.1. Detection of foreign chemical groups by ATR-FTIR

Figure 8.2 compares the FTIR spectra of the alginate films. The molecular vibrations that correspond to the peaks in the spectra were identified as listed in Table 8.1.

All of the chemical groups that were identified could be explained by the structure of the alginate molecule. That is, the presence of foreign molecules was not detected in the spectra. Furthermore, when the peak shapes and intensities were examined at high magnification, no obvious differences were found between the spectra of each of the purified alginates, nor between the purified and crude alginate spectra.

If contaminants were present in the samples, then their effect on the alginate molecules was undetectable to FTIR. Considering that the estimated concentrations of proteins, endotoxins, and polyphenols totaled to < 1.2% w/w, it is plausible that the quantity of impurities was simply too small to be detected by this technique.

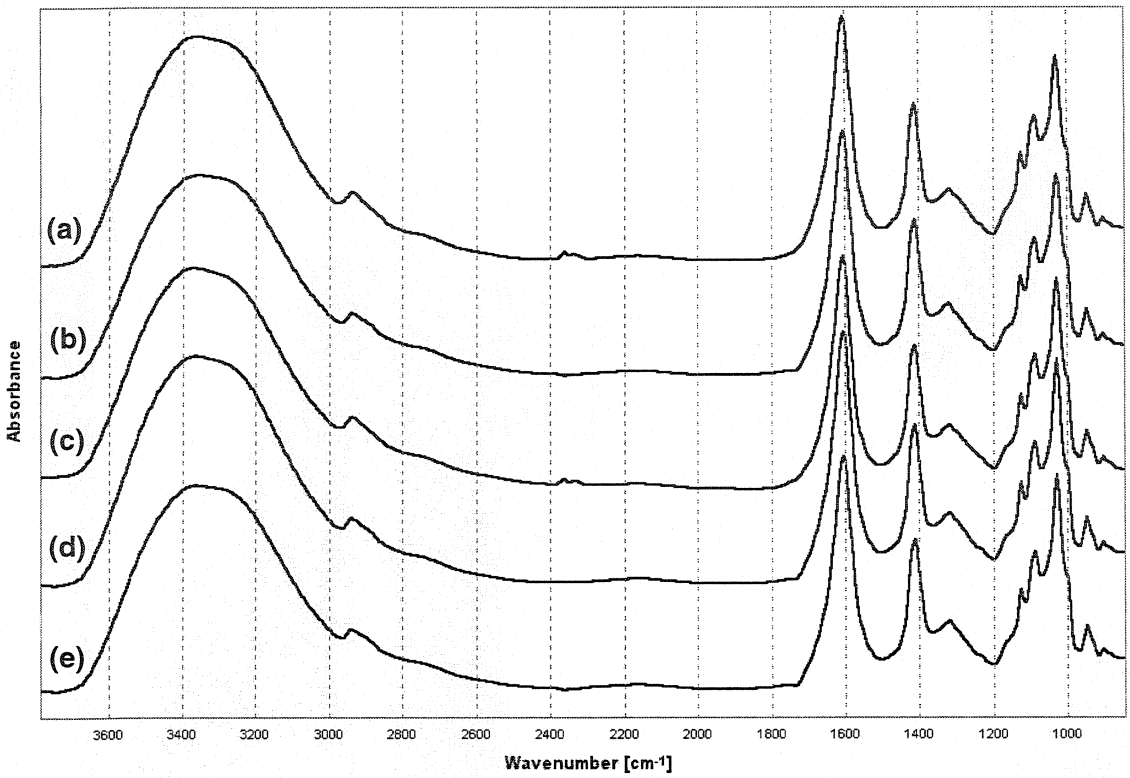


Figure 8.2: Comparison of the ATR-FTIR spectra of sodium alginate films. The films were cast from solutions (2% w/v) of the alginates (a) Crude, (b) PurKm, (c) PurWm, (d) PurDV, and (e) Pronova.

Table 8.1: Identification of peaks in the FTIR spectra of sodium alginate films.

Peak wavelength [cm^{-1}]	Assigned molecular vibration
3370 s,b*	OH stretch (intramolecular H-bond)
3250 s,b	OH stretch (intermolecular H-bond)
2940 w	CH stretch
1605 s	COO^- stretch (asymmetric)
1415 s	COO^- stretch (symmetric)
1320 m	CO stretch
1125 w	CC stretch (symmetric) + CO stretch
1090 m	CO stretch + CCO bend + CC bend
1025 s	CO stretch + CC stretch + COH bend
950 w	CO stretch + CCH bend

* s = strong, m = medium, w = weak, b = broad

8.2.2. Identification of foreign elements by XPS in survey mode

Table 8.2 lists the elemental compositions of the alginate films, as calculated from the XPS survey spectra. Hydrogen was not included in the compositions because the XPS technique is not sensitive to this element.

In terms of atomic percentage, all of the samples were composed of approximately 50% carbon, 40% oxygen, and 9% sodium. Theoretically, an alginate molecule is composed of 46% carbon, 46% oxygen, and 8% sodium. Thus, the films contained a slight excess of carbon and sodium, and/or a deficiency of oxygen. Since the composition of the crude alginate deviated the most from theoretical values, it can be reasoned that the excess carbon and sodium were contaminating the samples.

Furthermore, all of the purified alginate films contained traces of contaminating elements, including sulphur, phosphorus, nitrogen, fluorine, and silicon.

Sulphur was detected in all of the purified alginates, in concentrations of 0.3 - 0.7%. The crude alginate also contained sulphur, indicating that this element contaminated the samples before the purification process. It is possible that the sulphur originated from the disulfide bonds found in some protein types. A negligeable correlation between the sulphur and protein contents (R = 0.16), however, suggested otherwise. The other plausible explanation for the presence of sulphur is that fucoidans, i.e. sulphated polysaccharides that exist naturally in the cell walls of algae, were contaminating the alginate.

Phosphorus, in concentrations of 0.02 – 0.12%, was detected in all of the purified alginates. This element appeared to have contaminated the alginates before the purification process, as the control also contained phosphorus. Given that a major component of the endotoxin structure contains a phosphate group (Bishop 2004), the phosphorus most likely originated from these contaminants. Supporting this view is a strong correlation that was found between the phosphor and endotoxin concentrations (R

= 0.83). Furthermore, the extremely small concentrations of phophorus agreed with the endotoxin concentrations, which were estimated to be << 1% of the alginate's dry weight.

Nitrogen could be detected in two of the purified alginates, PurWM and PurDV, in quantities of 0.2% and 1.2%. This element was also found in the alginate before purification. Because the correlation between the nitrogen and protein concentrations was very strong (R = 0.96), and given that this element is an integral component of amino acids, it is highly probable that the nitrogen originated from contaminating proteins. What's more, the small concentrations of nitrogen agreed with the estimate that < 1% of the alginate's dry weight was composed of proteins.

For a single case, fluorine was detected in the alginate PurWm. This element was not once detected in the crude alginate, thus the fluorine contaminated the alginate either during or after the purification process. While it is possible that the film was contaminated by Teflon® tweezers (which contains CF_2) during sample handling, this contaminant was not found in any of the other alginates that were handled under the same experimental conditions.

Silicon was detected for a few trials, but this was due to exposure of the silicon substrate rather than impurities in the alginate film.

Overall, the total atomic percentage of foreign elements in a given purified alginate was never more than 2%. Furthermore, any observed differences between the purified alginates and the control, in terms of concentration of a contaminating element, were not statistically significant.

Table 8.2: Elemental compositions of sodium alginate films as measured by XPS (survey scan). The values represent the mean atomic percentage of a detected element ± SEM. A '0' indicates that the element was not detected in any of the trials.

		Crude	PurKm	PurWm	PurDV	Pronova
Native Elements	% C	53.5 ± 0.8	49.7 ± 3.6	50.5 ± 1.9	49.9 ± 1.1	51.2 ± 0.1
	% O	37.0 ± 1.2	40.2 ± 0.4	40.2 ± 0.3	39.2 ± 1.9	38.3 ± 0.6
	% Na	7.3 ± 0.9	9.4 ± 3.4	8.6 ± 2.1	9.0 ± 0.4	10.1 ± 0.8
Foreign Elements	% S	0.78 ± 0.23	0.67 ± 0.55	0.28 ± 0.17	0.48 ± 0.05	0.37 ± 0.13
	% P	0.06 ± 0.03	0.02 ± 0.02	0.12 ± 0.12	0.08 ± 0.07	0.03 ± 0.02
	% N	1.03 ± 0.47	0	0.16 ± 0.08	1.17 ± 0.63	0
	% Cl	0.11 ± 0.06	0	0	0	0
	% F	0	0	0.12 ± 0.12	0	0
	% Si	0.15 ± 0.15	0.07 ± 0.07	0	0.09 ± 0.09	0

8.2.3. Identification of foreign chemical groups by XPS in high resolution mode

The C_{1s}, O_{1s}, and Na_{1s} peaks of the XPS spectra were scanned at high resolution then deconvoluted into smaller peaks, which were subsequently labeled C_1 - C_5, O_1 - O_3, and Na_1 - Na_2. The chemical groups in which the carbon, oxygen, and sodium atoms were involved were identified by the binding energies of the peaks, as shown in Table 8.3. Table 8.4 shows the calculated atomic percentages of the elements in each chemical state.

The majority of the carbon, oxygen, and sodium atoms that were detected in the films belonged to chemical groups that could be associated with the alginate. Specifically, an average of 84% of the atoms contained in the purified samples were associated with the chemical groups COONa, C-O-C, O-C-O, and C-OH (corresponding to the peaks C_2, C_3, O_1, O_2, and Na_1) that exist naturally in sodium alginate molecules.

The other 16% of the film's compositions were associated with foreign chemical groups (corresponding to the peaks labeled C_1, C_4, C_5, O_3, and Na_2).

The chemical group corresponding to peak C_1 was identified as a saturated hydrocarbon, C-C. Relatively large quantities of these hydrocarbons were detected in the purified samples, contributing to 9 - 12% of their composition. The C-C quantities were too great to attribute their presence entirely to proteins, endotoxins, and polyphenols, which were estimated to total < 1.2 % of the alginate's weight. It was thus reasoned that most of the C-C groups belonged to a layer of adventitious hydrocarbons that adsorbed onto the film surface. With XPS, it is common to detect hydrocarbon adsorption on samples that have been exposed to the atmosphere. Plus, if the adsorbed layers were several angstroms thick, then their detected concentrations would expectedly be quite large. Still, the control contained higher amounts of C-C than the purified samples, implying that a small portion of the C-C groups originated from contaminants within the bulk of the alginate.

The chemical group corresponding to peak C_4, representing ~2% of the sample composition, was identified as a carboxyl acid group, COOH. It is probable that this

chemical group derived from contaminating proteins, as the COOH group is an integral component of amino acids. A strong correlation between the protein and COOH concentrations (R = 0.82) supports this hypothesis. However, it was estimated that the alginates contained < 1% proteins, so there was probably an additional source for the carboxylic acid group. If, during chemical processing, the alginic acid was not completely neutralized to the sodium salt, then the alginate molecule might still contain some COOH groups. A negative correlation (R = -0.72) between the carboxylic acid group and the COONa group (corresponding to Na_1) supports the hypothesis that insufficient neutralization contributed to the presence of COOH.

The chemical groups corresponding to peaks C_5 and O_3 were identified as carbon dioxide and water vapour, respectively. Each of these gases, which are prominent in the atmosphere, presumably adsorbed onto the film surface. In support of this view, the concentrations of these chemical groups were very similar between the purified samples and the control. Together, these species represented ~ 3% of the sample composition.

A sodium-containing group, corresponding to peak Na_2 and representing 1 – 5% of the sample composition, could not be identified. The probability that it originated from NaCl is low because of a discrepancy in the corresponding binding energy with the literature, and because chlorine was not detected in any of the purified alginates. A comparison with the control suggests that this impurity was introduced during the purification process.

To verify that the peaks labeled C_1, C_4, C_5, O_3, and Na_2 corresponded to contaminating species, the atomic compositions of the samples were recalculated using only the peaks that were associated with the alginate molecule (peaks C_2, C_3, O_1, O_2, and Na_1). As shown in Figure 8.3, the relative atomic percentages of the carbon, oxygen, and sodium in the alginate films approached theoretical values when the selected chemical groups were excluded, confirming their identification as impurities.

Overall, any differences that were observed between the sample compositions were not statistically significant.

Table 8.3: Chemical groups at the surface of sodium alginate films as detected by XPS (high resolution scan). The groups were identified by the presence of spectral peaks (labeled C_x, O_x, and Na_x) at characteristic binding energies. Peaks marked with an asterisk (*) were associated with contamination.

	Peak Label	Binding Energy [eV]	Assigned Chemical Group
C_{1s}	C_1*	285.0	C-C saturated hydrocarbon
	C_2	286.8	C-O-C , C-OH
	C_3	288.3	O-C-O , COONa
	C_4*	289.8	COOH
	C_5*	291.0	CO_2 adsorbed
O_{1s}	O_1	531.6	COONa
	O_2	533.1	C-O
	O_3*	534.5	H_2O adsorbed
Na_{1s}	Na_1	1071.7	COONa
	Na_2*	1072.7	Na-?

Table 8.4: Chemical composition of sodium alginate films as measured by XPS (high resolution scan). The chemical groups associated with each peak (labeled C_x, O_x, and Na_x) are identified in Table 8.3. The values represent the mean atomic percentage of the element in the chemical group ± SEM. Peaks marked with asterisk (*) were associated with contamination.

		Crude	PurKm	PurWm	PurDV	Pronova
C_{1s}	% C_1*	15.1 ± 3.2	8.5 ± 1.3	10.2 ± 2.5	10.5 ± 4.9	11.7 ± 3.3
	% C_2	27.0 ± 4.0	29.1 ± 7.3	27.8 ± 6.5	26.2 ± 4.2	26.4 ± 5.4
	% C_3	10.3 ± 1.1	10.1 ± 0.2	10.6 ± 1.3	12.0 ± 1.1	11.1 ± 1.3
	% C_4*	2.0 ± 0.5	1.8 ± 0.6	1.9 ± 0.8	2.0 ± 0.4	1.7 ± 0.2
	% C_5*	1.5 ± 0.4	1.6 ± 0.5	1.6 ± 0.6	1.7 ± 0.3	1.8 ± 0.4
O_{1s}	% O_1	10.4 ± 1.4	10.3 ± 3.1	10.6 ± 3.1	12.8 ± 1.4	11.8 ± 2.4
	% O_2	24.9 ± 4.3	29.1 ± 3.7	28.5 ± 4.7	26.0 ± 4.3	26.6 ± 3.6
	% O_3*	2.6 ± 1.6	1.2 ± 0.8	1.8 ± 1.2	1.3 ± 0.1	1.1 ± 0.2
Na_{1s}	% Na_1	4.6 ± 1.6	6.9 ± 1.1	6.3 ± 0.7	6.2 ± 1.3	6.2 ± 1.7
	% Na_2*	0.5 ± 0.9	4.9 ± 0.6	2.7 ± 0.1	0.8 ± 0.1	1.9 ± 0.4

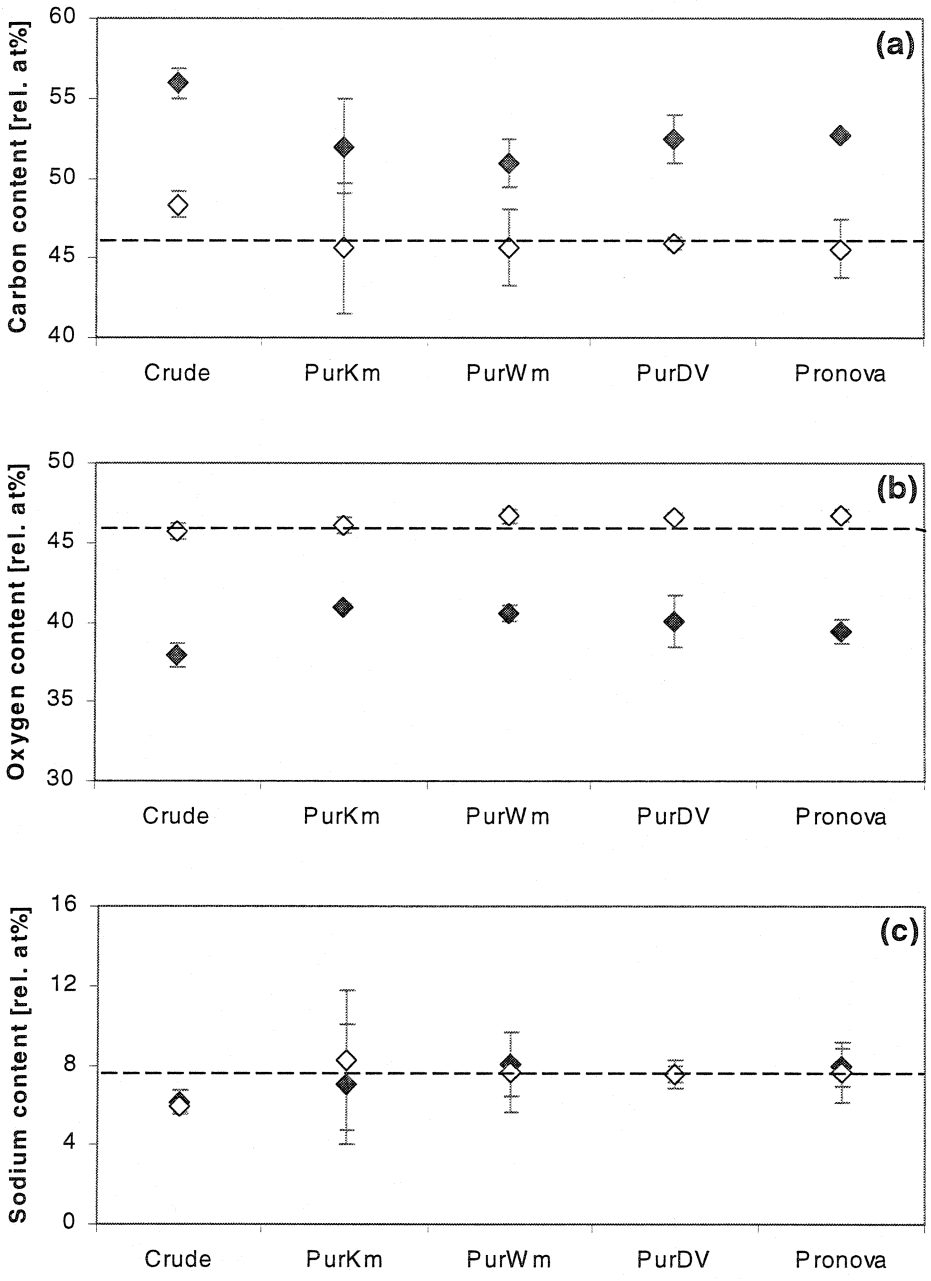


Figure 8.3: The relative contents of **(a)** carbon, **(b)** oxygen, and **(c)** sodium in alginate films. Values are expressed as the mean atomic percentage ± SEM. The filled diamonds (◆) represent values measured directly from XPS spectra (high resolution scan). The open diamonds (◇) represent values that were recalculated after excluding chemical groups presumed to be contaminating the samples. The dashed line represents the theoretical contents as calculated from the molecular structure of sodium alginate.

8.3. Indirect detection of contaminants

8.3.1. Effect on solution viscosity

The viscosities of the alginates solutions at 2% w/v concentration are shown in Figure 8.4. This relative order of viscosities was consistent for concentrations from 1.5% to 2.5% w/v. The viscosities at these concentrations can be found in the Appendix C.

Three of the four purified alginate solutions were more viscous than the control. This suggests that purifying the alginates induced an increase in their solution viscosities. There are several possible explanations for the observed increase in viscosity:

The first explanation is that purifying the alginates augmented their average molecular weights. This may have been possible if small fragments of low molecular weight alginate were eliminated during the purification process.

On the other hand, the removal of contaminants could have slowed the degradation rate of the alginates. Considering that polyphenols are suspected to induce degradation (Skjak-Braek G. et al. 1989), this is a plausible explanation. Though, a weak correlation between the polyphenol contents and the solution viscosities ($R = -0.4$) suggests that this was not the principal factor.

The alternative explanation is that the removal of contaminants allowed the alginate chains to fully extend in the solution, increasing their hydrodynamic volume. This implies that the contaminants altered the natural conformation of the alginate molecules, by promoting intramolecular bonding and hindering the interaction of the alginate with the solvent. This scenario is very likely, as it is supported by negative correlations between impurity contents and solution viscosities. In particular, the presence of proteins and endotoxins tended to coincide with lower viscosities ($R = -0.5$). The presence of the COOH group also correlated with lower viscosities ($R = -0.7$).

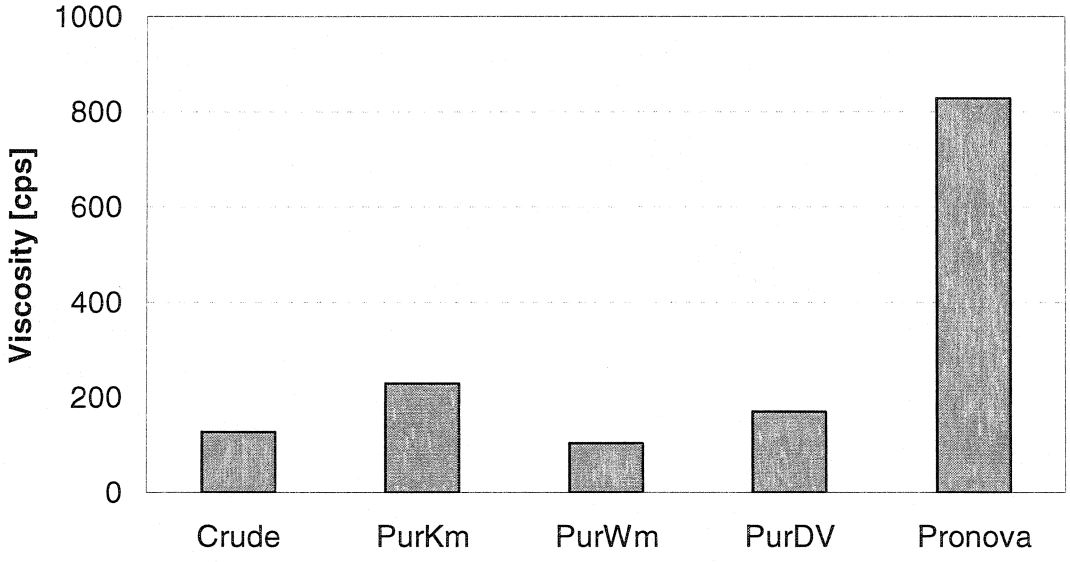


Figure 8.4: Measured dynamic viscosity of sodium alginate solutions (2% w/v). Note that 1 cps = 1 mPa·s.

8.3.2. Effect on thermal behaviour

As shown in Figure 8.5, the measured glass transition temperatures of the purified alginate films ranged from 103°C to 107°C.

All of the purified samples had lower glass transition temperatures than the control, suggesting that purifying the alginates increased the mobility of the polymer chains. There are a few plausible explanations for the observed decrease in glass transition temperature:

The first explanation is that purifying the alginates decreased their chain length. It has been suggested that multi-step processes for chemical purification can induce sample degradation (Prokop and Wang 1997), so, on one hand, this situation is plausible. On the other hand, this scenario directly contradicts the results of the viscosity experiments.

Alternatively, the removal of the contaminants could have increased the flexibility of the alginate chain so that they required less energy (i.e. heat) to move freely. This implies that the contaminants bonded with the alginate molecules in a manner that hindered their freedom to move. This situation is the likelier because it agrees with results of the viscosity measurements. It is also supported by a positive correlation between the contamination levels of the alginates and their glass transition temperatures. Specifically, the proteins, endotoxins, and polyphenols all correlated with a decrease in alginate mobility ($R = 0.55$ to 0.8). As well, the presence of the COOH group appeared to have a strong impact on the thermal behaviour of the alginates ($R = 0.9$).

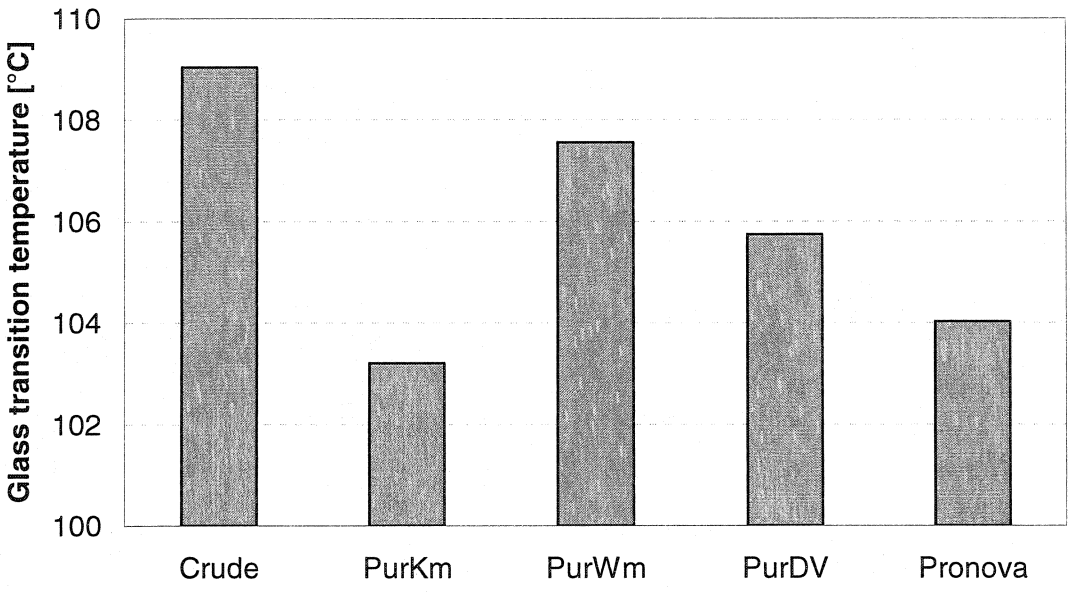


Figure 8.5: Glass transition temperature of sodium alginates as measured by DSC. Measurements were made during a second heating (20°C/min).

8.3.3. Effect on wettability

The left contact angles of water on the alginates films are shown in Figure 8.6. Because the surface was horizontal, the right contact angles were identical (data not shown). The contact angles on the purified alginate films ranged from 31° to 42°. These values were significantly lower than the contact angle for the crude alginate ($p < 0.001$). This implies that purifying the alginates increased the hydrophilicity of their film surfaces.

In general, the increased hydrophilicity indicates that a greater number of hydrophilic (i.e. polar) groups were exposed at the sample surface. Theoretically, an alginate molecule contains two hydrophilic groups, the COO^-Na^+ and C-OH groups, that interact with water molecules. A strong negative correlation between the detected amount of COONa groups and the contact angles ($R = -0.9$) confirms that this relationship also existed experimentally.

The contamination levels of the alginates correlated positively with the measured contact angles, implying that the impurities discouraged the exposure of the hydrophilic groups. In particular, protein and polyphenol contents correlated strongly with the measured contact angles ($R = 0.8$ to 0.9), as did the presence of the COOH group ($R = 0.9$). A moderate correlation between the sulphur content and the contact angle also existed ($R = 0.6$). These contaminants could have bonded directly to the COO^- and C-OH groups and/or they could have altered the conformation of the alginate molecules so that the hydrophilic groups were hidden from the water molecules. Either situation agrees with the viscosity and DSC results.

It should be noted that since the contact angle technique is surface sensitive, the adsorption layer on the film surfaces would conceivably have influenced the results. In fact, all surfaces exposed to a gaseous atmosphere adsorb hydrophobic molecules in order to lower their surface energy. A strong correlation between the amount of saturated C-C bonds and the contact angles ($R = 0.9$) supports the suspicions that surface contamination contributed to the observed increases in sample hydrophobicity.

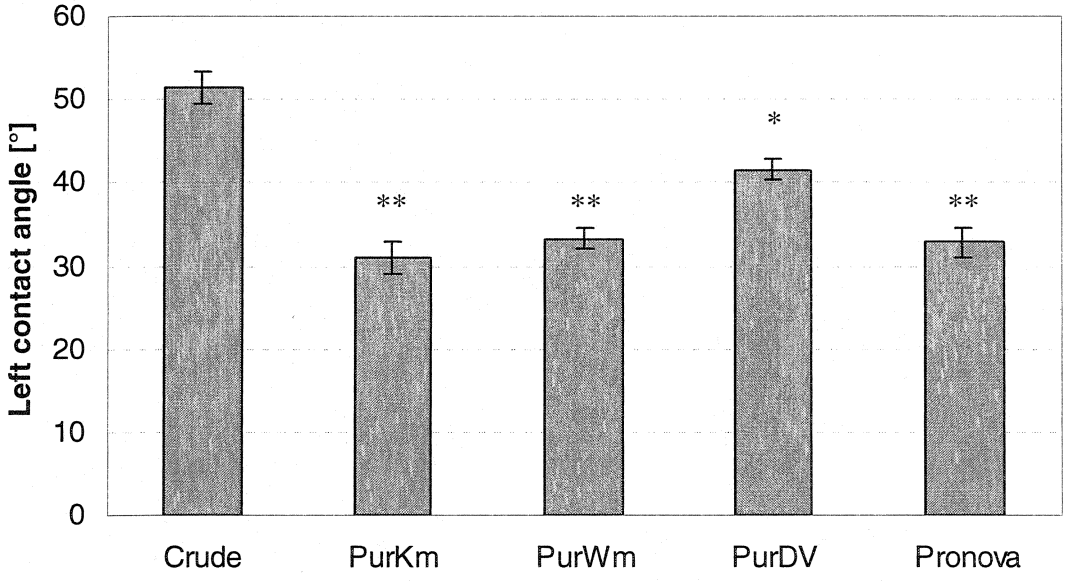


Figure 8.6: Measured contact angles of water on sodium alginate films 10s after contact. Values are expressed as the mean ± SEM. * $p < 0.001$, ** $p < 0.0001$ when compared to crude alginate.

8.4. *In vivo* evaluations of alginate bioreactivity

8.4.1. Free-floating immune cells

As Figure 8.7 shows, between 3.3 and 4.4 million free-floating immune cells were counted in the peritoneal fluid of the mice two days after barium alginate beads were implanted into their peritoneal cavities. After 14 days implantation, the number of free-floating cells was much smaller, ranging from 0.5 to 1.4 million cells.

Statistically, purifying the alginate had no significant effect on the number of free-floating immune cells that were counted in the peritoneal fluid.

Nevertheless, the contamination levels of the alginates correlated negatively with the number of free-floating immune cells that were detected two days after implantation. This does not necessarily imply that the contaminated alginates attracted less immune cells to the implantation site. Rather, a negative correlation ($R = -0.9$) between the number of free-floating cells and the degree of cell adhesion to the bead surfaces (refer to section 8.4.2) suggests that the contaminated alginates stimulated the recruited immune cells to adhere to the bead surface rather than remain free-floating. As Table 8.5 shows, the proteins and endotoxins, along with the COOH group, appeared to have the most pronounced effect on the number of free-floating immune cells.

After 14 days implantation, the effect of alginate contamination on the number of free-floating immune cells was no longer obvious.

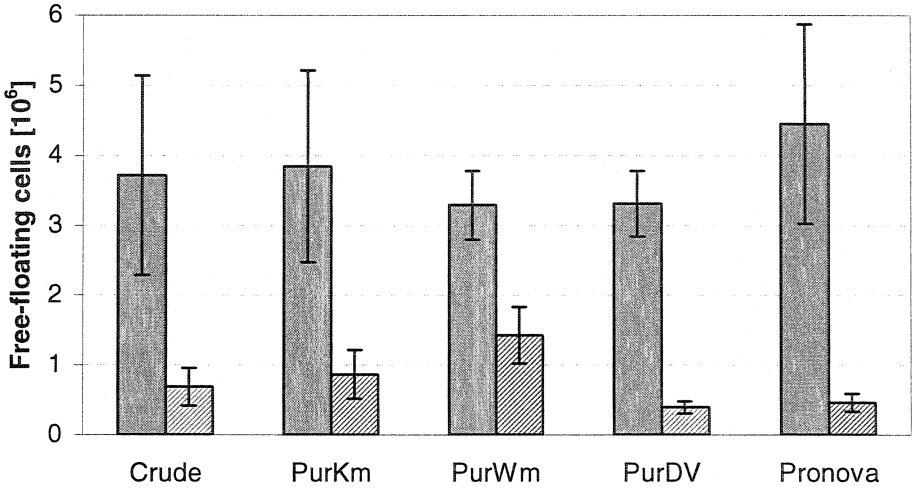


Figure 8.7: Number of immune cells that were free-floating in the peritoneal liquid of mice after barium alginate beads were implanted into their peritoneal cavities. The solid bars represent the cell count after 2 days implantation, and the diagonally striped bars represent the cell count after 14 days implantation. The values are expressed as the mean ± SEM.

Table 8.5: Correlation between various properties of sodium alginate and the number of free-floating immune cells that were found 2 and 14 days after bead implantation. The values represent the correlation coefficient R.

		2 days	14 days
Common Contaminants	Proteins	-0.63	-0.36
	Nitrogen	-0.51	-0.43
	Endotoxins	-0.58	0.81
	Phosphorus	-0.78	0.56
	Polyphenols	-0.10	-0.16
Other Impurities	COOH	-0.71	0.08
	Sulphur	0.08	-0.31
	Sodium [Na-?]	0.15	0.47
Alginate Properties	Concentration	-0.83	0.36
	Chain stiffness [Tg]	-0.52	0.30
	Hydrophobicity [CA]	-0.26	-0.33

8.4.2. Pericapsular reaction

As Figure 8.8 shows, the mean score describing the pericapsular reaction after two days implantation ranged from 0.3 to 1.4. After 14 days implantation, the bead surfaces were more thoroughly covered by adhered cells, as the scores increased to a range of 1.4 to 1.8.

Purifying the alginates had a considerable effect on the severity of the pericapsular reaction. That is, each of the purified samples had scores that were significantly smaller than the control after 2 days implantation. After 14 days implantation, two of the purified samples had significantly smaller scores.

As Table 8.6 shows, the contamination levels of the alginates correlated positively with the severity of the pericapsular reaction around the implanted beads. This implies that the foreign body reactions were induced, at least in part, by the presence of the contaminants. While almost all of the identified contaminants appeared to increase the severity of the pericapsular reaction after 2 days implantation, the presence of polyphenols and the COOH group seemed to have a particularly strong effect on the reaction. After 14 days implantation, the relationship between the foreign body reaction and the presence of proteins, polyphenols, and the COOH group became even more pronounced.

Moreover, it was observed that the more hydrophilic alginates correlated with less severe pericapsular reactions. As Table 8.6 shows, this relationship was apparent after two days implantation, and very strong after 14 days implantation. This effect was not entirely unexpected, as most proteins adsorb in higher amounts to hydrophobic rather than hydrophilic surfaces (Holmberg 2002). Accordingly, proteins that promoted immune cell adhesion could have adsorbed more readily to the hydrophobic surfaces of the contaminated beads. A more specific explanation, which was recently described in the literature (Morra and Cassinelli 2000), is that water molecules were bound so strongly to the hydrophilic surfaces that the cell-adhesive proteins could not displace them in order to adsorb to the beads. That is, non-specific adsorption of the proteins was perhaps resisted by the formation of a protective interfacial layer of water.

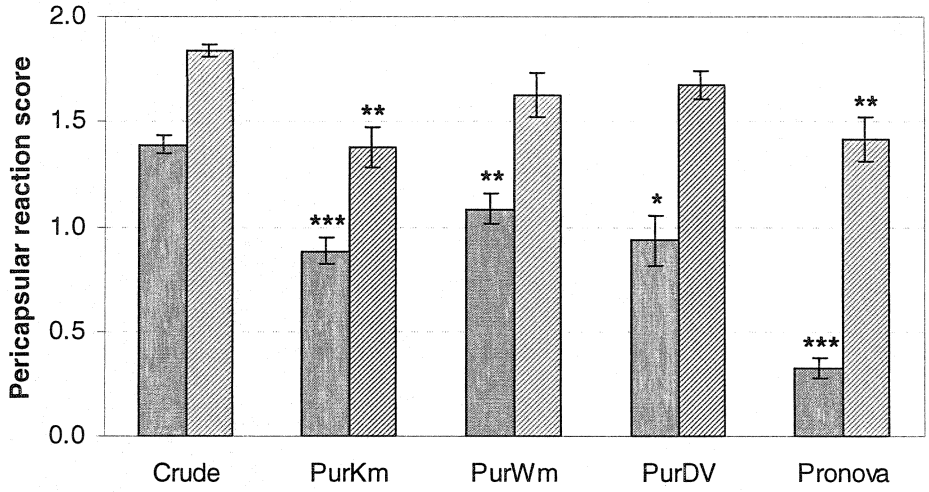


Figure 8.8: Severity of the pericapsular reaction around barium alginate beads that were retrieved 2 days (solid bars) and 14 days (diagonally striped bars) after implantation in the peritoneal cavity of mice. The values are expressed as the mean reaction score ± SEM. * $p < 0.05$, ** $p < 0.01$, *** $p < 0.001$ when compared to the crude alginate.

Table 8.6: Correlation between various properties of sodium alginate and the severity of the pericapsular reaction that was evaluated 2 and 14 days after bead implantation. The values represent the correlation coefficient R.

		2 days	14 days
Common Contaminants	Proteins	0.50	0.79
	Nitrogen	0.58	0.84
	Endotoxins	0.59	0.53
	Phosphorus	0.42	0.54
	Polyphenols	0.71	0.80
Other Impurities	COOH	0.87	0.98
	Sulphur	0.51	0.29
	Sodium [Na-?]	-0.24	-0.77
Alginate Properties	Concentration	0.97	0.86
	Chain stiffness [Tg]	0.79	0.93
	Hydrophobicity [CA]	0.67	0.90

8.4.3. Adhered Immune Cells

As Figure 8.9 shows, the average number of immune cells that were adhered to the implant surface ranged from 200 to 3500 per bead after two days implantation. After 14 days implantation, the numbers appeared to decrease to a range of 130 to 1740 cells per bead.

It was observed that, after 14 days implantation, a significant amount of fibrotic tissue surrounded the beads. During the digestion process to recover the adhered cells, the presence of this tissue and other debris interfered with the results by masking immune cells so that they could not be counted. As a consequence, the results give the impression that the number of adhered cells decreased over the implantation period. These results, however, are not representative of the immunogenicity of the beads and were thus not considered for further analysis.

After two days implantation, the purified samples tended to accumulate a smaller number of immune cells at their surfaces. Though, the observed differences in the numbers were not statistically significant.

As Table 8.7 shows, the contamination levels of the alginates correlated positively with the number of immune cells that adhered to the beads after two days implantation. The polyphenols and the COOH group were most strongly associated with the accumulation of adhered cells, though the proteins, endotoxins, and sulphur content also appeared to have an effect.

As before, it was observed that the more hydrophilic alginates produced beads that induced weaker immune reactions after two days implantation. This effect can again be explained by the tendency for hydrophilic surfaces to resist protein adsorption.

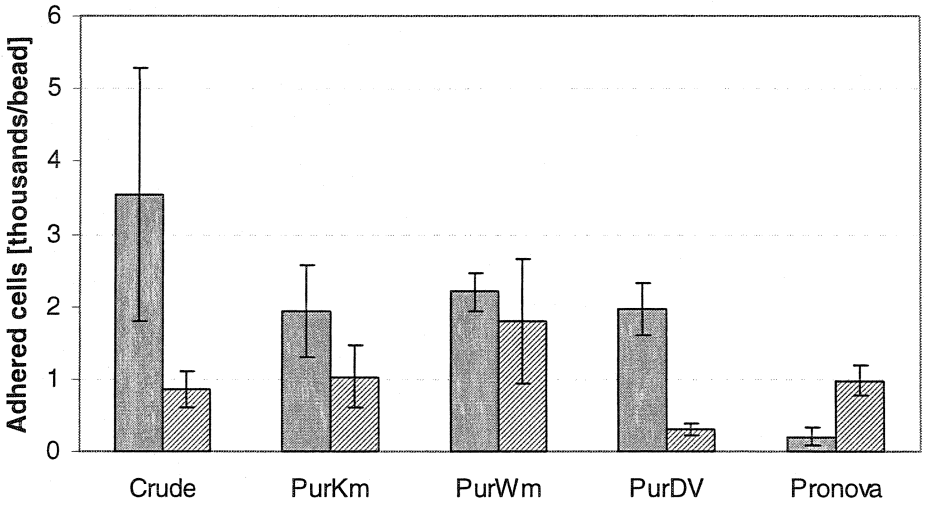


Figure 8.9: Number of immune cells that were adhered to the surfaces of barium alginate beads after 2 days (solid bars) and 14 days (diagonally striped bars) implantation in the peritoneal cavity of mice. The values are expressed as the mean number cells per bead that were adhered to the surface ± SEM.

Table 8.7: Correlation between various properties of sodium alginate and the number of immune cells that were adhered to the bead surfaces 2 days after bead implantation. The values represent the correlation coefficient R.

Common Contaminants	Proteins	0.49
	Nitrogen	0.60
	Endotoxins	0.50
	Phosphorus	0.30
	Polyphenols	0.77
Other Impurities	COOH	0.86
	Sulphur	0.62
	Sodium [Na-?]	-0.25
Alginate Properties	Concentration	0.94
	Chain stiffness [Tg]	0.76
	Hydrophobicity [CA]	0.72

8.5. Chemical composition of the microcapsule surface

8.5.1. FTIR measurements

Based on the experimental conditions for the ATR-FTIR measurements, it was estimated that the penetration depth of the infrared beam into the sample ranged from 0.2 to 3 μm, depending on the specific frequency (refer to Appendix D). Therefore, it must be assumed that the FTIR spectrum of the microcapsules represents the chemical composition of the outermost 3 μm of the dehydrated samples.

Figure 8.10 compares the ATR-FTIR spectrum of the dehydrated APA microcapsules to the spectra of sodium alginate films, PLL films, and dehydrated calcium alginate gel beads. The molecular vibrations associated with the spectral peaks were identified and are listed in Table 8.8. Note that the small peak near 2350 cm^{-1} corresponds to carbon dioxide gas in the atmosphere and was therefore ignored in the analyses.

The FTIR spectrum of the microcapsules displayed all of the absorbance bands that were characteristic of alginate, indicating that alginate was a principal substance at the microcapsule surface. The peaks at 1605 cm^{-1} and 1415 cm^{-1}, which correspond to the COO^- groups in the alginate, were shifted to slightly lower wavenumbers in the microcapsule spectrum compared to the film spectrum. This reflects that the chemical environment around the ionized carboxyl group was altered. This was probably an effect of the sodium ions being replaced by other ions that differed in mass and/or affinity for the COO^- group, the most likely candidates being the NH_3^+ groups of the poly-L-lysine or the Ca^{2+} ions from the gel core. Additionally, the peaks at 1025 cm^{-1} and 950 cm^{-1} were shifted to higher frequencies in the microcapsule spectrum, which indicates that the strengths of the C-O and C-C bonds in the carbohydrate rings were slightly altered, possibly due to conformational changes.

The microcapsule spectrum also contained the strongest of the peaks that were characteristic of poly-L-lysine. Specifically, the absorbance bands associated with Amide A, Amide I, and Amide II vibrations were detected at the microcapsule surface. These bands arise from the N-H stretching, N-H bending, C=O stretching, and C-N stretching vibrations of the amide group in the polypeptide. The amide A band of the microcapsule spectrum was at a higher wavenumber than for the PLL spectrum, indicating that the N-H stretching of the amide was more weakly hydrogen-bonded in the microcapsule than in the film. Furthermore, the placement of the Amide I and II bands in the spectra is directly related to the conformation of the polypeptide. Accordingly, three conformations of the molecule were present in the PLL film: α-helix (1650 and 1540 cm^{-1}), unparallel β-sheet (1625 and 1520 cm^{-1}), and random coil (1660 and 1550 cm^{-1}). An inspection of the microcapsule spectrum at high magnification revealed the presence of weak shoulders that correspond to these amide bands. The relative intensity of the absorbance bands indicated that the PLL, as a microcapsule component, was mostly in the α-helix and random coil conformations, and to a lesser extent, in the β-sheet conformation.

There were no obvious indications of calcium alginate being present at outermost portions of the microcapsules.

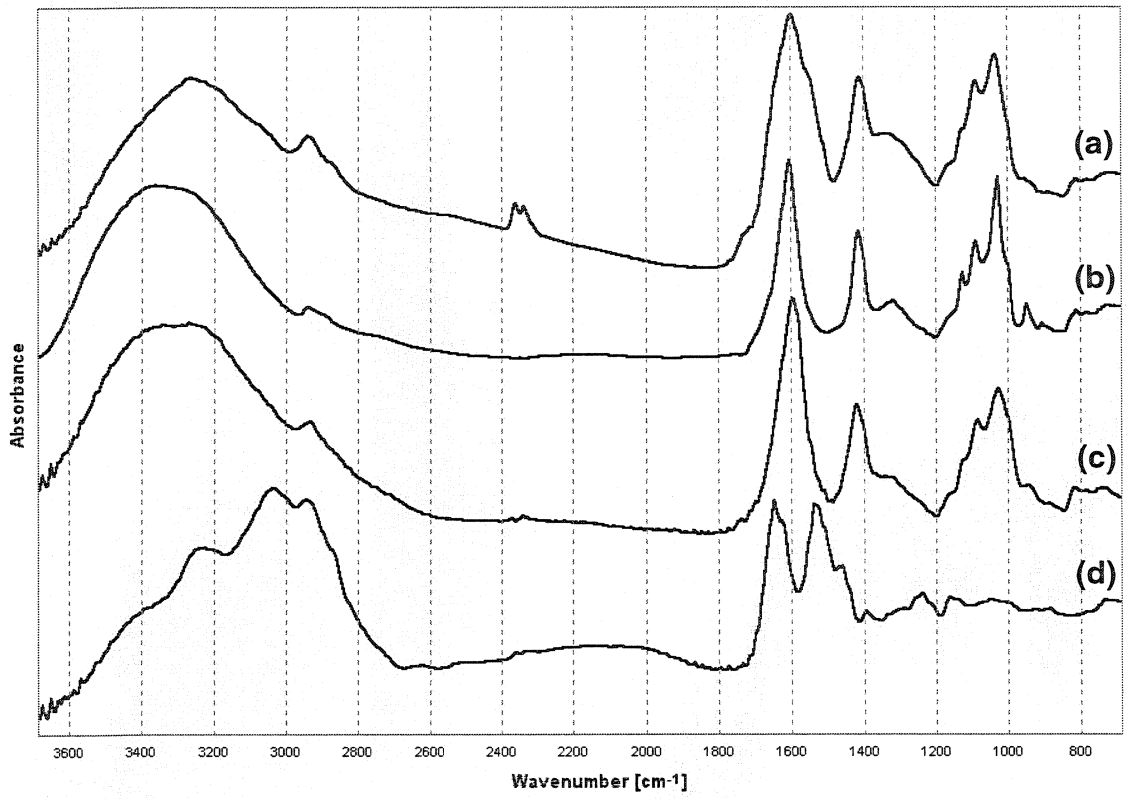


Figure 8.10: ATR-FTIR spectra of (a) dehydrated APA microcapsules, (b) sodium alginate film, (c) dehydrated calcium alginate gel beads, and (d) poly-L-lysine film. The peaks in the spectrum have been identified in Table 8.8.

Table 8.8: Assignment of FTIR absorbance bands for APA microcapsules, sodium alginate films, poly-L-lysine films, and calcium alginate gel beads. The values represent the wavenumber [cm^{-1}] of the spectral peak.

Capsule	Alginate	PLL	Ca gel bead	Peak Assignment
3370 s,b	3370 s,b		3370 s,b	OH stretch (intramolecular H-bond)
3265 s				Amide A
	3250 s,b		3250 s,b	OH stretch (intermolecular H-bond)
		3235 m		Amide A
		3040 s		NH_3 stretch (asymmetric)
		2940 s		CH stretch + NH_3 stretch (symmetric)
2940 w	2940 w		2930 w	CH stretch + CH_2 stretch (asymmetric)
2875 sh		2870 sh		CH_2 stretch (symmetric)
		1660 sh		Amide I (random coil)
		1650 s		Amide I (α helix) + NH_3 bend (asymmetric)
1645 sh				Amide I
		1625 sh		Amide I (β sheet)
1595 s	1605 s		1595 s	COO- stretch (asymmetric)
1555 sh				Amide II
		1550 sh		Amide II (random coil)
		1540 s		Amide II (α helix)
		1520 sh		Amide II (β sheet)
		1470 m		NH3 bend (symmetric)
		1460 m		CH_2 bend
1410 s	1415 s		1420 s	COO- stretch (symmetric)
		1395 w		CO stretch
1320 m	1320 m		1320 m	CO stretch
		1240 w		CH_2 wag + CH_2 twist
		1160 w		C-N stretch
1125 w,sh	1125 w		1125 w,sh	CC stretch (symmetric) + CO stretch
1090 m	1090 m		1085 m	CO stretch + CCO bend + CC bend
1030 s	1025 s		1025 s	CO stretch + CC stretch + COH bend
955 w	950 w		945 w	CO stretch + CCH bend

s = strong, m = medium, w = weak, b = broad, sh = shoulder

8.5.2. XPS measurements

The XPS technique analyzes photoelectrons that are emitted from the outermost 20 - 100 Å of the sample. Therefore, it must be assumed that the XPS spectra of the microcapsules represent the chemical composition of the outermost 100 Å of the dehydrated samples.

The elemental compositions of the dehydrated microcapsules, sodium alginate films, poly-L-lysine films, and the dehydrated calcium alginate gel beads were calculated from the XPS spectra scanned in survey mode. The results are presented in Table 8.9.

The microcapsule surface was primarily composed of carbon, oxygen, and nitrogen, and small amounts of sodium. In addition, traces of chlorine were detected for one trial. It was reasoned that the chlorine originated from the NaCl solution that was used for the fabrication of the microcapsules. Silicon was also detected, but this was attributed to exposure of the silicon substrate rather than the film composition. While sulphur and phosphorus could not be detected at the microcapsule surface, the relatively intense silicon-related peaks would have hidden their presence if their quantities were too small.

The microcapsule surface contained far less sodium than the alginate. This result supports the earlier suggestions (refer to section 8.5.1) that a portion of the sodium ions was replaced when the alginate formed a microcapsule layer. Since no calcium was detected at all, it is most likely that the replacement ions were the NH_3^+ groups of the PLL.

Moreover, nitrogen was detected at the microcapsule surface. Since this element represented almost 5% of the capsule composition, it's improbable that it derived solely from protein contamination in the alginates. It is much more plausible that poly-L-lysine was the main source of nitrogen.

Figure 8.11 compares the ratios of carbon to oxygen, to sodium, and to nitrogen that were calculated for each of the samples. The C/O ratio of the microcapsule was significantly higher than that of the alginate, yet noticeably lower than that of the PLL, suggesting that

the microcapsule surface contained a mixture of both substances. There was also a significant difference between the C/Na ratios of the microcapsule and the alginate. On the other hand, the C/N ratio of the microcapsule was only slightly higher than the C/N ratio of the PLL. This suggests that more PLL was present than alginate. The relative presence of PLL and alginate could be estimated by dividing the C/N ratio of the PLL by the C/N ratio of the microcapsule, and similarly with the C/Na ratio for the alginate. From these calculations, it was estimated that 81% of the carbon atoms detected at the microcapsule surface originated from PLL, while 16% of the carbon belonged to alginate.

An examination of the C_{1s} peak at high resolution shows that the microcapsule contained not only the alginate-associated carbons (C-O, C-OH, O-C-O, COONa), but also carbons that belong to the PLL molecule (C-C, C-N, C=O). The relative concentrations of the carbon belonging to each the alginate and PLL could not be calculated because overlapping peaks could not be separated. However, it was estimated from the peak heights that 55% of the carbon was associated with PLL and 45% with alginate. While these values differ from the percentages that were estimated by dividing the C/N and C/Na ratios, it confirms that the majority of the carbons that were detected at the microcapsule exterior belonged to PLL rather than alginate.

Similarly, the O_{1s} peak of the microcapsule spectrum indicated the presence of the C-O and COONa groups of the alginate, as well as the C=O group of the PLL. Again, overlapping peaks could not be deconvoluted, so the exact contributions of PLL and alginate could not be clearly defined. Nevertheless, it was estimated that 30% of the oxygen atoms were associated with PLL and the remaining with alginate. Given that the O/C ratio of alginate is, theoretically, 3 times greater than the O/C ratio of PLL, the estimated contributions of oxygen atoms from the alginate and PLL are consistent with the estimates from the C_{1s} peak analysis.

The N_{1s} peak for the microcapsule was almost identical in shape and energy to that for the PLL, confirming that the nitrogen principally originated from the PLL molecule.

Table 8.9: Surface elemental compositions of APA microcapsules and their components, as measured by XPS (survey scan). The values are expressed as the mean atomic percentage of the element ± SEM. A '0' indicates that the element was not detected for any of the trials.

	Capsule	Alginate	Poly-L-lysine	Ca Gel Bead
% C	55.9 ± 0.3	51.2 ± 0.1	60.1 ± 3.2	35.0 ± 0.9
% O	32.1 ± 0.7	38.3 ± 0.6	27.9 ± 2.5	34.7 ± 0.9
% Na	1.8 ± 0.3	10.1 ± 0.8	0	0
% N	4.54 ± 0.07	0	7.57 ± 3.41	0.17 ± 0.09
% S	0	0.37 ± 0.13	0	0
% P	0	0.03 ± 0.02	0	0
% Cl	0.05 ± 0.05	0	0	0
% Br	0	0	3.7 ± 1.5	0
% Ca	0	0	0	0.6 ± 0.1
% Si	5.7 ± 1.2	0	0.8 ± 0.8	29.5 ± 0.2

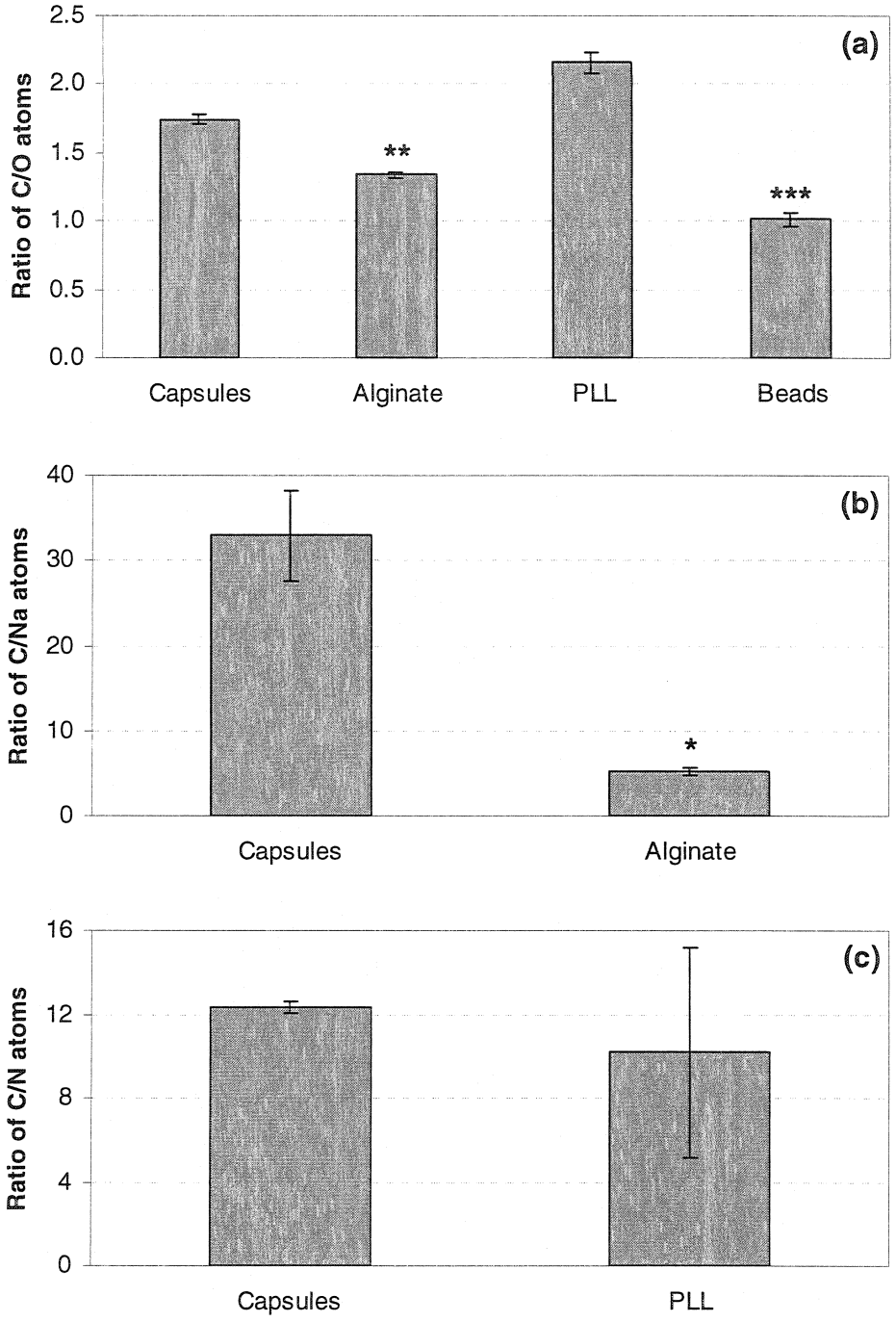


Figure 8.11: Comparison of the elemental composition of APA microcapsules with their components, as calculated by XPS (survey scan), and in terms of the (a) C/O ratio, (b) C/Na ratio, and (c) C/N ratio. The values are expressed as the mean ratio of the atomic percents ± SEM. * $p < 0.05$, ** $p < 0.01$, *** $p < 0.001$ when compared to the capsules.

8.5.3. ToF-SIMS analysis

In the TOF-SIMS technique, < 10 Å of the sample surface is sputtered and analyzed. Thus, it is assumed that the microcapsule spectrum from this analysis represents the chemical composition of the outermost monolayer of the sample.

Figure 8.12 compares the positive ion mass spectrum of the microcapsule surface with the spectra of sodium alginate and PLL films. Because XPS showed no evidence of calcium alginate at the microcapsule surface, the gel beads were not analyzed using ToF-SIMS. Table 8.10 lists the ions that were detected at the microcapsule surface.

Since the intensity of a peak in a mass spectrum is generally not proportional to the analyte concentration, it was not possible to quantify the relative amounts of alginate and PLL at the microcapsule surface. It was, however, possible to deduce which ions derived from alginate or PLL. This was achieved by comparing the precise masses (i.e. spectral peak positions) of the ions that were sputtered from the different samples, as shown in Table 8.10.

There were several ions above 60 Da that were sputtered from the microcapsule surface, which were also characteristic of the alginate molecule. Many of them were identified as sodium-containing fragments, such as Na_2OH^+ and $C_3O_2Na^+$. Moreover, large fragments (m = 479, 501, and 517) that also appeared in the alginate mass spectrum were detected at the microcapsule surface. Their large masses suggest that the fragments consisted of several intact alginate monomers.

Many ions that were characteristic of PLL were also detected at the microcapsule surface. In particular, many lower mass ions containing nitrogen were sputtered from the sample surface, including NH_2^+, NH_3^+, and $C_xH_xN^+$. None of the higher mass ions above 150 Da, however, were associated with PLL, indicating that no large fragments of the PLL molecule were sputtered from the microcapsule surface.

In addition to alginate and PLL, traces of calcium were also found at the microcapsule surface (m = 40). It is unlikely that the detected calcium originated from the exposed gel core of the microcapsule because calcium was also detected as a trace contaminant in the alginate and PLL samples.

As well, Na_2Cl^+ was detected from the microcapsules, supporting the suspicion that the chlorine traces that were detected by XPS originated from a salty substance.

A number of ions that were sputtered from the microcapsule surface, particularly the heavier ions weighing over 100 Da, could not be attributed to the presence of alginate or PLL molecules. Since these ions were primarily composed of C, O, H, Na, and N, it is plausible that they originated from alginate-PLL complexes that formed during the microcapsule fabrication. This would explain why they could not be found in the spectra of the individual alginate and PLL films. Moreover, this view agrees with earlier results that suggested close interactions between the alginate and PLL molecules.

Overall, the ion mass spectra of the samples suggest that the outermost monolayer of the microcapsule surface contained not only alginate, but also PLL. Though, it could not be determined whether intact molecules of PLL were at the surface, or only PLL fragments and alginate-PLL complexes.

The ion mass spectrum of the microcapsule represents the chemical composition of a 50 μm × 50 μm area of the surface. The reconstructed images of this surface area are shown in Figure 8.13. These images display the precise locations from which the detected ions originated. It is evident from these images that the area of analysis was homogeneous in chemical composition. Therefore, the possibility that the PLL was detected at the surface due to inconsistencies in the outer alginate coating was rejected.

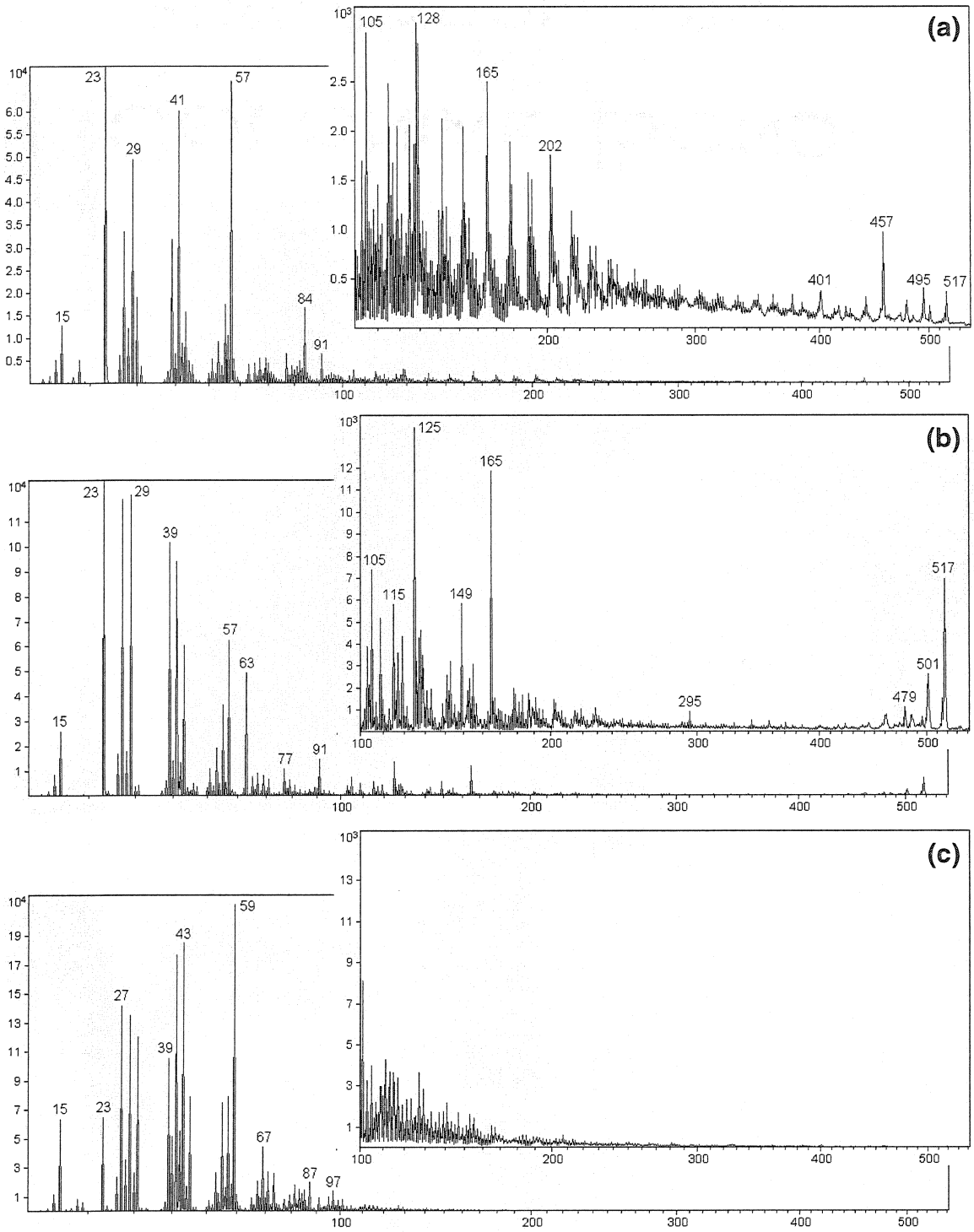


Figure 8.12: Positive ion mass spectra of the **(a)** APA microcapsule surface, **(b)** alginate film, and **(c)** PLL film, as measured by ToF-SIMS. The x axes represent the ion mass [m/z] and the y axes represent the count intensity. The upper right-hand boxes are magnified views (~ ×10) of the mass spectra between 100 and 540 m/z.

Table 8.10: Identification of positive ions that were sputtered from the surface of an APA microcapsule. A × signifies that the ion was also sputtered from the alginate or PLL.

Ion Mass	Assignment	Alginate	PLL	Ion Mass	Assignment	Alginate	PLL
1.01	H	×	×	65.04	C_5H_5	×	×
2.02	H_2	×	×	66.04	C_5H_6	×	×
12.00	C	×	×	67.05	C_5H_7	×	×
13.01	CH	×	×	68.05	C_4H_6N		
14.02	CH_2	×	×	68.93	^69Ga	×	×
15.02	CH_3	×	×	69.03	C_4H_5O	×	×
17.03	NH_3		×	69.07	C_5H_9	×	×
18.03	NH_4		×	70.07	C_4H_8N		×
22.99	Na	×	×	75.02	C_6H_3	×	
26.02	C_2H_2	×	×	76.99	CHO_4		
27.02	C_2H_3	×	×	77.04	C_6H_5	×	×
28.02	CH_2N	×	×	78.04	C_6H_6	×	×
28.03	C_2H_4	×	×	79.05	C_6H_7	×	×
29.00	CHO	×	×	80.05	C_5H_6N		
29.04	C_2H_5	×	×	80.95	Na_2Cl		
30.04	CH_4N		×	81.03	C_5H_5O	×	×
31.02	CH_3O	×	×	81.07	C_6H_9	×	×
31.04	CH_5N		×	82.07	C_5H_8N		×
37.01	C_3H	×	×	84.09	C_5H_10N		×
38.02	C_3H_2	×	×	89.04	C_7H_5	×	
38.98	Unknown			90.98	C_3O_2Na	×	
39.02	C_3H_3	×	×	91.06	C_7H_7	×	×
39.96	Ca	×	×	93.07	C_7H_9		×
40.03	C_3H_4	×	×	94.07	C_6H_8N		×
41.04	C_3H_5	×	×	95.06	C_5H_7N_2		
42.01	C_2H_2O	×	×	96.09	SiH_12N_4		
42.03	C_2H_4N	×	×	98.10	C_6H_12N		
42.04	C_3H_6	×	×	103.05	C_8H_7	×	×
43.02	C_2H_3O	×	×	105.07	SiC_2H_11N_3	×	×
43.04	C_2H_5N		×	115.05	C_9H_7	×	×
43.06	C_3H_7	×	×	117.05	C_3H_7N_3O_2		
44.05	C_2H_6N		×	124.95	SiCONa_3		
45.03	C_2H_5O	×	×	127.05	C_6H_9Na_2	×	
45.06	C_2H_7N		×	128.06	C_8H_9Na	×	
50.01	C_4H_2	×	×	129.06	C_6H_9O_3		×
51.02	C_4H_3	×	×	141.06	Si_2C_6H_13		
52.03	C_4H_4	×	×	152.05	C_4H_12O_4Si		
53.00	C_3HO	×	×	153.05	C_9H_10Cl		
53.04	C_4H_5	×	×	165.07	C_9H_11Na_2	×	
54.03	C_3H_4N		×	178.05	C_13H_6O		
54.05	C_4H_6	×	×	189.04	C_5H_7N_3O_5		
55.02	C_3H_3O	×	×	191.06	C_14H_7O		
55.05	C_4H_7	×	×	202.06	C_12H_10O_3		
56.05	C_3H_6N		×	215.06	C_11H_12O_3Na		
57.03	C_3H_5O	×	×	401.20	C_18H_34O_8Na		
57.07	C_4H_9	×	×	457.26	C_20H_41O_11		
58.07	C_3^13CH_9	×		478.87	Unknown	×	
59.05	C_3H_7O	×	×	495.29	Unknown		
62.98	Na_2OH	×		501.24	Unknown	×	
63.02	C_5H_3	×	×	517.27	Unknown	×	

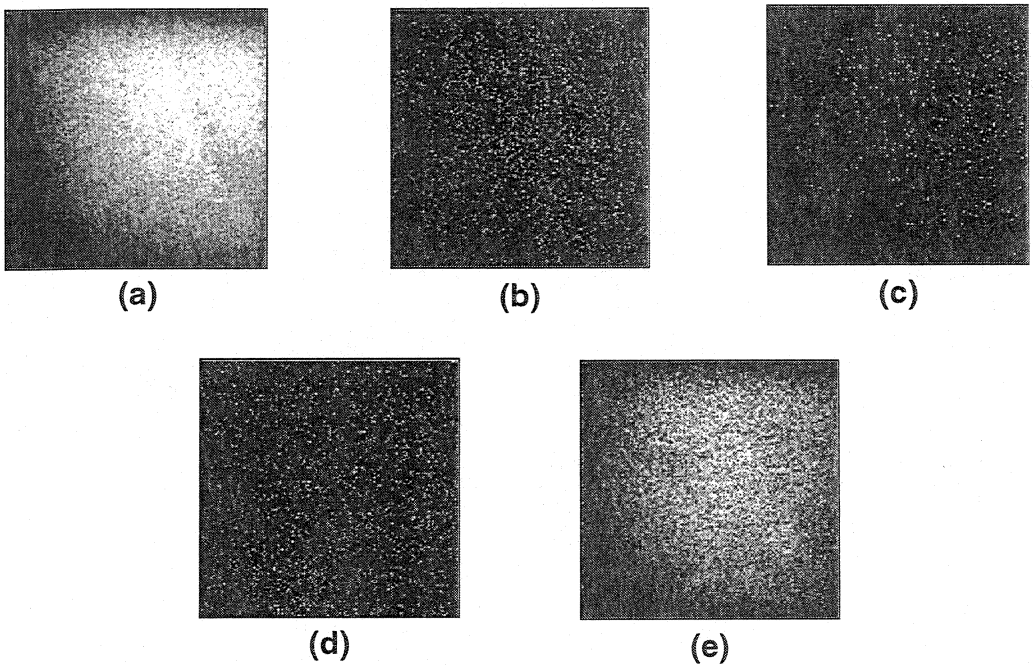


Figure 8.13: Images of a 50 μm × 50 μm area of the microcapsule surface, as reconstructed from the ion mass spectra measured by ToF-SIMS. The images represent the locations and concentrations of **(a)** all detected ions, **(b)** Na_2OH^+ (m = 63) that is representative of alginate, **(c)** $C_4H_8N^+$ (m = 70) that is representative of PLL, **(d)** calcium (m = 40), and (e) sodium (m = 23). The lighter areas indicate a higher concentration of the ion.

CHAPTER 9: CONCLUDING REMARKS

9.1. Experimental conclusions

9.1.1. Alginate contamination

It was clearly demonstrated that the commercially available sodium alginates contained contaminants. What's more, these contaminants could not be completely eliminated by chemical means. Even after purification, as much as 7% of the alginate's atomic composition could be attributed to bulk contaminants.

Proteins, endotoxins, and polyphenols were among the residual contaminants. Additionally, traces of sulphur, which presumably originated from fucoidans, as well as a sodium-containing compound, contaminated the samples. The alginates also contained carboxylic acid groups that originated from proteins and/or insufficiently neutralized portions of the alginate molecule.

9.1.2. Effect of contaminants on biocompatibility

The identified contaminants undoubtedly contributed to the immunogenicity of the alginate gel beads. Specifically, proteins, polyphenols, and, to a lesser extent, endotoxins appeared to promote the adhesion of immune cells to the bead surface. In addition, the presence of COOH groups seemed to have a particularly potent effect on the severity of foreign body reactions. The contaminating sulphur and sodium, however, had no obvious impact on bioreactivity of the gels.

The evidence suggested that, in addition to being immunogenic, the contaminants were indirectly contributing to immunogenicity of the implants. That is, the contaminants proved capable of altering the natural conformation and hydrophilicity of the alginate molecules via bonds with the COO^- and C-OH groups. This might have interfered with

the alginate's abilities to resist the adsorption of proteins that promote immune cell adhesion to the bead surface.

9.1.3. Chemical composition of the microcapsule surface

It was repeatedly demonstrated that both PLL and alginate exist near the microcapsule surface. Within the outermost 100Å of the microcapsules, it was estimated that over 50% of the carbon content originated from the PLL while the rest was attributed to alginate. Moreover, it was shown that the outermost monolayer of the microcapsules contained molecules and/or fragments of both alginate and PLL.

The evidence suggested that, as a membrane component, the PLL was primarily bound to the alginate to form an alginate-PLL complex. It was confirmed that membrane formation was based on interactions between the NH_3^+ groups of the PLL and the COO^- groups of the alginate, and involved at least two conformations (α-helix, random coil, and maybe β-sheet) of the PLL molecule. A portion of the surface alginate, however, retained its sodium ions and hence may not have been bound to the PLL. Even so, PLL exposure did not appear to be due to defects or inconsistencies in the outer alginate coating.

9.2. Limitations of this research project

Understanding and improving the biocompatibility of APA microcapsules is a very ambitious goal that in reality requires the combined efforts of several research groups over many years. With this consideration in mind, it can be acknowledged that this research project had its limitations to the number of issues that it could resolve. While many of these limitations were imposed by experimental, economical, and time constraints, some may still be overcome in future studies.

- Because organic impurities are similar in composition to alginates, a few contaminants could not be explicitly identified. In the future, techniques such as

Maldi-TOF, that are specific to the study of organic samples, may be useful for resolving this issue.

- In order to avoid the trigger of immune reactions by morphological defects, it was necessary to control the solution viscosity during bead fabrication. As a result, the beads contained varying alginate concentrations. The results indicated that the concentration had an observable effect on the bead biocompatibility, making it difficult to directly correlate contamination levels with immunogenicity. Though, since the quantity of impurities increases proportionally with alginate concentration, it can still be concluded that contamination was the principal trigger for the reactions.
- Due to experimental constraints, it was not possible to study the microcapsules in their hydrated state. Because polymers can be very dynamic, then the surface state of the dehydrated microcapsule may not be the same as the surface state of an implanted microcapsule. In the future, the application of techniques, such as atomic force microscopy, that can examine the microcapsule surface while it is immersed in a fluid would provide some interesting information to complement this project.

9.3. Summary of original contributions

Before this project, the chemical composition of purified commercial alginates has never been studied so extensively. By applying physicochemical techniques as well as standard bioassays, it was discovered that, in addition to proteins, endotoxins, and polyphenols, alginates also contain a number of previously undetected impurities.

Moreover, this was the first clear demonstration that chemical purification does not completely remove these contaminants. Since even minute concentrations of these impurities can have a profound effect on the *in vivo* biocompatibility of the alginates, this may explain why, despite chemical purification of the alginates, other research groups observe foreign body reactions against beads and capsules.

This project showed for the first time that contaminants are capable of altering the conformation and hydrophilicity of alginate molecules. The hypothesis that contaminants can trigger an immune reaction by interfering with the alginate's natural biocompatibility is hence both novel and original.

For the first time, the chemical composition of the top atomic layer of the microcapsules was directly investigated. As a result, this project provided the first physical evidence of PLL exposure at the true microcapsule surface.

9.4. Recommendations for future research

Based on the new evidence provided by this project, it is recommended that the biocompatibility of the alginates be optimized using two approaches:

The first approach is to completely eliminate all immunogenic impurities from the alginates. Since it was established that it is not sufficient to assess purity levels using only standard bioassays, it is recommended that physicochemical techniques, such as the ones that were used in this project, be applied to ensure that the alginates are consistently free of all contaminants. Finding an economical method for producing such highly purified alginates, however, may not be straightforward.

This leads to the second suggested method for improving alginate biocompatibility. This approach consists of counteracting the effects that the contaminants have on the alginate properties. If, in fact, the immunogenicity of the alginates is principally due to the altered conformation and hydrophilicity of the molecule, then it may not be necessary to eliminate 100% of the contaminants. For example, a plasma treatment could be used to increase the hydrophilicity of the alginates enough to render the polymer fully biocompatible.

Based on the new, direct evidence of PLL exposure at the microcapsule surface, it is recommended, with justification, that efforts to improve PLL coverage be continued.

Given that the PLL exposure did not appear to result from defects or inadequate binding of the alginate coating, it is suggested that the thickness of the outer alginate layer be increased. This can possibly be achieved by increasing the concentration of the alginate solution during microcapsule fabrication, or by cross-linking the alginates with calcium ions to form a thick gel layer.

Furthermore, it is advisable that new microcapsule designs be screened for PLL exposure using physicochemical techniques, such as XPS and ToF-SIMS, before implanting them into animal models, as this approach would be most ethical and cost-efficient.

REFERENCES

AMERICAN DIABETES ASSOCIATION. 2004. "All About Diabetes: Type 1 Diabetes". In *American Diabetes Association web-site*. [On line]. http://www.diabetes.org/type-1-diabetes.jsp (Page consulted August 2004)

BISHOP, R.E. 2004. "Fundamentals of Endotoxin Structure and Function". In *Department of Laboratory Medicine and Pathobiology, University of Toronto web-site*. [On line]. http://www.utoronto.ca/LabMedPathobiology/education/undergraduate/lmp%20436/Bishop.pdf (Page consulted August 2004)

BRETZEL, R.G., ECKHARD, M., BRENDEL, M.D. 2004. "Pancreatic islet and stem cell transplantation: new strategies in cell therapy of diabetes mellitus". *Panminerva Med.* 46:1. 25-42.

CALAFIORE, R. 2002. "Bioartificial Pancreas". *Polymeric Biomaterials*. Edited by DUMITRIU S. New York : Marcel Dekker, Inc. P. 983-1006.

CHAPLIN, M. 2004. "Alginate". In *Water Structure and Behaviour*. [On line]. http://www.lsbu.ac.uk/water/hyalg.html (Page consulted August 2004)

CLAYTON, H.A., LONDON, N.J., COLLOBY, P.S., BELL, P.R., JAMES, R.F. 1991. "The effect of capsule composition on the biocompatibility of alginate-poly-l-lysine capsules". *J Microencapsul.* 8:2. 221-33.

COOPER, J.F. 2003. "The Necessity Of Reliable Endotoxin Standards". In *Charles River Laboratories Technical Documents*. [On line]. http://www.criver.com/techdocs/documents/LAL_Times_Dec98_000.pdf (Page consulted August 2004)

DE VOS, P., DE HAAN, B., VAN SCHILFGAARDE, R. 1997a. "Effect of the alginate composition on the biocompatibility of alginate-polylysine microcapsules". *Biomaterials*. 18:3. 273-8.

DE VOS, P., DE HAAN, B.J., WOLTERS, G.H., STRUBBE, J.H., VAN SCHILFGAARDE, R. 1997b. "Improved biocompatibility but limited graft survival after purification of alginate for microencapsulation of pancreatic islets". *Diabetologia*. 40:3. 262-70.

DE VOS, P., HOOGMOED, C.G., BUSSCHER, H.J. 2002. "Chemistry and biocompatibility of alginate-PLL capsules for immunoprotection of mammalian cells". *J Biomed Mater Res* . 60:2. 252-9.

ERTESVAG, H., VALLA, S. 1998. "Biosynthesis and applications of alginates". *Polymer Degradation and Stability*. 59:85-91.

FAN, M.Y., LUM, Z.P., FU, X.W., LEVESQUE, L., TAI, I.T., SUN, A.M. 1990. "Reversal of diabetes in BB rats by transplantation of encapsulated pancreatic islets". *Diabetes*. 39:4. 519-22.

FMC BIOPOLYMER. 2004. "FMC Alginates". In *FMC Biopolymer web-site*. [On line]. http://www.fmcbiopolymer.com (Page consulted August 2004)

FRITSCHY, W.M., DE VOS, P., GROEN, H., KLATTER, F.A., PASMA, A., WOLTERS, G.H. et al. 1994. "The capsular overgrowth on microencapsulated pancreatic islet grafts in streptozotocin and autoimmune diabetic rats". *Transpl Int.* 7:4. 264-71.

HOLMBERG, K. 2002. "Control of Protein Adsorption at Surfaces". *Encyclopedia of Surface and Colloid Science*. Edited by HUBBARD A.T. Marcel Dekker, Inc. P. 1242-1253.

IHARA, H., MATSUMOTO, A., SHIBATA, M., HIRAYAMA, C. 2004. "Host-Guest Chemistry Using alpha-Helical Poly(L-lysine)". In *Applied Chemistry and Biochemistry, Kumamoto University web-site*. [On line]. http://www.chem.kumamoto-u.ac.jp/~ihara/article_pme96/text.html (Page consulted August 2004)

KING, A., SANDLER, S., ANDERSSON, A. 2001. "The effect of host factors and capsule composition on the cellular overgrowth on implanted alginate capsules". *J Biomed Mater Res*. 57:3. 374-83.

KLOCK, G., FRANK, H., HOUBEN, R., ZEKORN, T., HORCHER, A., SIEBERS, U. et al. 1994. "Production of purified alginates suitable for use in immunoisolated transplantation". *Appl Microbiol Biotechnol*. 40:5. 638-43.

KLOCK, G., PFEFFERMANN, A., RYSER, C., GROHN, P., KUTTLER, B., HAHN, H.J. et al. 1997. "Biocompatibility of mannuronic acid-rich alginates". *Biomaterials*. 18:10. 707-13.

KULSENG, B., SKJAK-BRAEK, G., FOLLING, I., ESPEVIK, T. 1996. "TNF production from peripheral blood mononuclear cells in diabetic patients after stimulation with alginate and lipopolysaccharide". *Scand J Immunol*. 43:3. 335-40.

KULSENG, B., SKJAK-BRAEK, G., RYAN, L., ANDERSSON, A., KING, A., FAXVAAG, A. et al. 1999. "Transplantation of alginate microcapsules: generation of antibodies against alginates and encapsulated porcine islet-like cell clusters". *Transplantation* . 67:7. 978-84.

LEINFELDER, U., BRUNNENMEIER, F., CRAMER, H., SCHILLER, J., ARNOLD, K., VASQUEZ, J.A. et al. 2003. "A highly sensitive cell assay for validation of purification regimes of alginates". *Biomaterials*. 24:23. 4161-72.

LIM, F., SUN, A.M. 1980. "Microencapsulated islets as bioartificial endocrine pancreas". *Science*. 210:4472. 908-10.

MANSKE, C.L. 1999. "Risks and benefits of kidney and pancreas transplantation for diabetic patients". *Diabetes Care*. 22 Suppl 2 :B114-20.

MORRA, M., CASSINELLI, C. 2000. "Force measurements on cell repellant and cell adhesive alginic acid coated surfaces". *Colloids Surf B Biointerfaces*. 18:3-4. 249-259.

MORRIS, P.J. 1996. "A critical review of immunosuppressive regimens". *Transplant Proc* . 28:6 Suppl 1. 37-40.

ORIVE, G., HERNANDEZ, R.M., RODRIGUEZ GASCON, A., CALAFIORE, R., CHANG, T.M., DE VOS, P. et al. 2004. "History, challenges and perspectives of cell microencapsulation". *Trends Biotechnol*. 22:2. 87-92.

ORIVE, G., PONCE, S., HERNANDEZ, R.M., GASCON, A.R., IGARTUA, M., PEDRAZ, J.L. 2002. "Biocompatibility of microcapsules for cell immobilization elaborated with different type of alginates". *Biomaterials*. 23:18. 3825-31.

OTTERLEI, M., OSTGAARD, K., SKJAK-BRAEK, G., SMIDSROD, O., SOON-SHIONG, P., ESPEVIK, T. 1991. "Induction of cytokine production from human monocytes stimulated with alginate". *J Immunother*. 10:4. 286-91.

OTTERLEI, M., SUNDAN, A., SKJAK-BRAEK, G., RYAN, L., SMIDSROD, O., ESPEVIK, T. 1993. "Similar mechanisms of action of defined polysaccharides and lipopolysaccharides: characterization of binding and tumor necrosis factor alpha induction". *Infect Immun*. 61:5. 1917-25.

PROKOP, A., WANG, T.G. 1997. "Purification of polymers used for fabrication of an immunoisolation barrier". *Ann N Y Acad Sci.* 831:223-31.

RAYAT, G.R., RAJOTTE, R.V., AO, Z., KORBUTT, G.S. 2000. "Microencapsulation of neonatal porcine islets: protection from human antibody/complement-mediated cytolysis in vitro and long-term reversal of diabetes in nude mice". *Transplantation* . 69:6. 1084-90.

SHAPIRO, A.M., LAKEY, J.R., RYAN, E.A., KORBUTT, G.S., TOTH, E., WARNOCK, G.L. et al. 2000. "Islet transplantation in seven patients with type 1 diabetes mellitus using a glucocorticoid-free immunosuppressive regimen". *N Engl J Med.* 343:4. 230-8.

SKJAK-BRAEK G. , MURANO E. , PAOLETTI S. 1989. "Alginate as Immobilization Material. II: Determination of Polyphenol Contaminants by Fluorescence Spectroscopy, and Evaluation of Methods for Their Removal". *Biotechnol Bioeng.* 33:90-94.

SMIDSROD, O., SKJAK-BRAEK, G. 1990. "Alginate as immobilization matrix for cells". *Trends Biotechnol.* 8:3. 71-8.

SOON-SHIONG, P., FELDMAN, E., NELSON, R., KOMTEBEDDE, J., SMIDSROD, O., SKJAK-BRAEK, G. et al. 1992. "Successful reversal of spontaneous diabetes in dogs by intraperitoneal microencapsulated islets". *Transplantation.* 54:5. 769-74.

SOON-SHIONG, P., HEINTZ, R.E., MERIDETH, N., YAO, Q.X., YAO, Z., ZHENG, T. et al. 1994. "Insulin independence in a type 1 diabetic patient after encapsulated islet transplantation". *Lancet.* 343:8903. 950-1.

STRAND, B.L., MORCH, Y.A., ESPEVIK, T., SKJAK-BRAEK, G. 2003. "Visualization of alginate-poly-L-lysine-alginate microcapsules by confocal laser scanning microscopy". *Biotechnol Bioeng.* 82:4. 386-94.

STRAND, B.L., RYAN, T.L., IN'T VELD, P., KULSENG, B., ROKSTAD, A.M., SKJAK-BREK, G. et al. 2001. "Poly-L-Lysine induces fibrosis on alginate microcapsules via the induction of cytokines". *Cell Transplant.* 10:3. 263-75.

SUN, Y., MA, X., ZHOU, D., VACEK, I., SUN, A.M. 1996. "Normalization of diabetes in spontaneously diabetic cynomologus monkeys by xenografts of microencapsulated porcine islets without immunosuppression". *J Clin Invest.* 98:6. 1417-22.

THE ISLET FOUNDATION. 2004. "One Way to Replace Islet Cells". In *The Islet Foundation web-site.* [On line]. http://www.islet.org/12.htm (Page consulted August 2004)

THU, B., BRUHEIM, P., ESPEVIK, T., SMIDSROD, O., SOON-SHIONG, P., SKJAK-BRAEK, G. 1996. "Alginate polycation microcapsules. I. Interaction between alginate and polycation". *Biomaterials.* 17:10. 1031-40.

VAN HOOGMOED, C.G., BUSSCHER, H.J., DE VOS, P. 2003. "Fourier transform infrared spectroscopy studies of alginate-PLL capsules with varying compositions". *J Biomed Mater Res.* 67A:1. 172-8.

WIJSMAN, J., ATKISON, P., MAZAHERI, R., GARCIA, B., PAUL, T., VOSE, J. et al. 1992. "Histological and immunopathological analysis of recovered encapsulated allogeneic islets from transplanted diabetic BB/W rats". *Transplantation.* 54:4. 588-92.

ZIMMERMANN, U., KLOCK, G., FEDERLIN, K., HANNIG, K., KOWALSKI, M., BRETZEL, R.G. et al. 1992. "Production of mitogen-contamination free alginates with variable ratios of mannuronic acid to guluronic acid by free flow electrophoresis". *Electrophoresis.* 13:5. 269-74.

APPENDICES

Appendix A: Commercial production of alginate

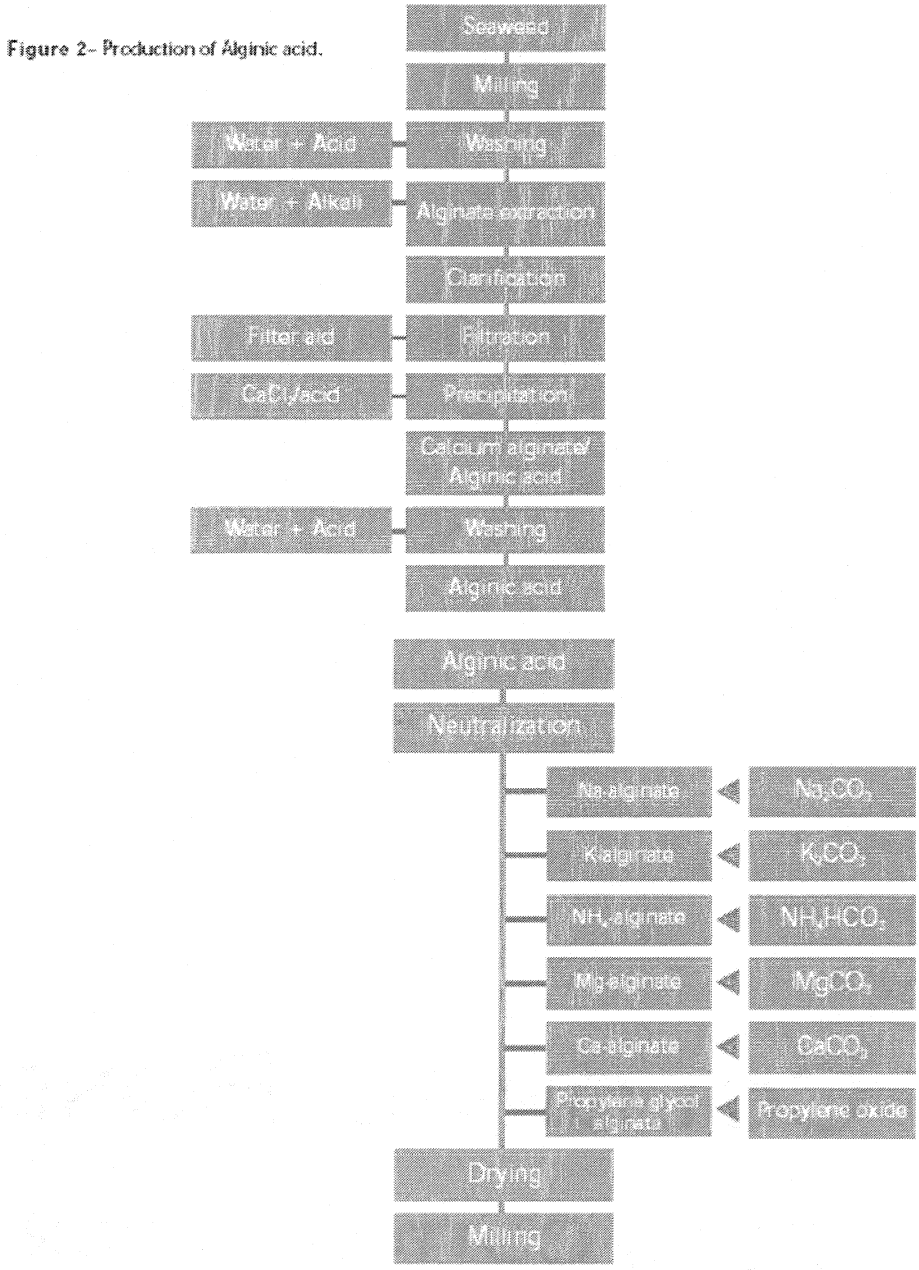


Figure 2- Production of Alginic acid.

Figure 3- Commercial salts and ester produced from Alginic acid supplied by FMC BioPolymer.

Figures are reproduced from (FMC BioPolymer 2004).

Appendix B: Specification sheet for Pronova™ UP LVG alginate

Product Specification Bulletin

NOVAMATRIX™
Ultrapure Polymer Systems

PRONOVA™ UP LVG

Generic name: Sodium alginate
Product no.:
Storage conditions: 3-8 °C
Packaging material: Duma, polyethylene containers

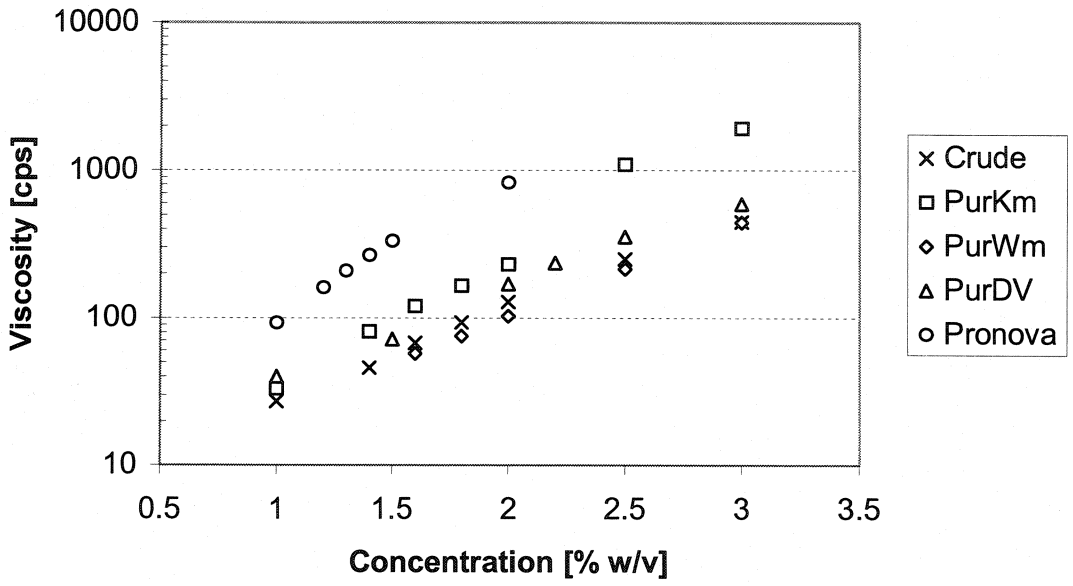
Parameter	Specification Range	Test Method
ID-test	Positive	AM-050
Appearance of powder	White to off-white	AM-057
Appearance of solution	Clear, colorless to slightly yellowish	AM-057
Apparent viscosity	20-200 mPa·s	AM-056
pH	5.5-8.5	AM-052
Dry matter content	≥ 85%	AM-001
Guluronic acid content	≥ 60%	AM-063
Protein content	≤ 0.3%	AM-051
Endotoxins	≤ 100 EU/g	AM-047
Heavy metals	≤ 40 ppm	AM-065
Pb	≤ 10 ppm	AM-017
Hg	≤ 1 ppm	AM-018
Total viable count	≤ 100 cfu/g	AM-062
Yeast and mould	≤ 100 cfu/g	AM-062

Abbreviations

AM: NovaMatrix standard method

Specification sheet was provided by NovaMatrix / FMC Biopolymer

Appendix C: Viscosities of alginate solutions



Appendix D: Penetration depth of ATR-FTIR

